

AD-A175 295

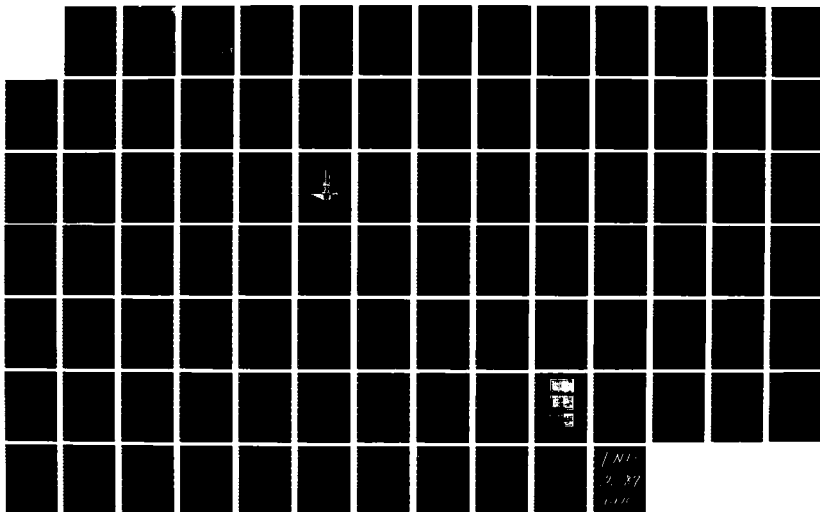
THE ULTRASONIC MEASUREMENT OF ELASTIC CONSTANTS OF  
CUBIC CRYSTALS(U) TENNESSEE UNIV KNOXVILLE DEPT OF  
PHYSICS M PURI DEC 86 TR-25 N00014-81-K-0229

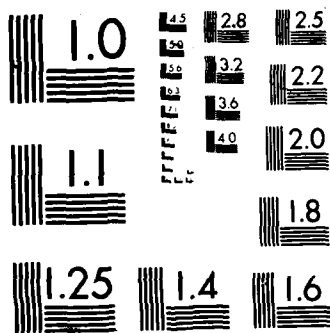
1/1

UNCLASSIFIED

F/G 20/2

NL





XERO COPY RESOLUTION TEST CHART

AD-A175 295

DEPARTMENT OF PHYSICS  
AND ASTRONOMY

OFFICE OF NAVAL RESEARCH  
CONTRACT NO. N00014-81-K-0229  
PROJECT NO. 384-306

M. A. Breazeale, Principal Investigator

THE ULTRASONIC MEASUREMENT OF ELASTIC  
CONSTANTS OF CUBIC CRYSTALS

by

Madhu Puri

DTIC  
ELECTE

DEC 18 1986

DTIC FILE COPY

**DISTRIBUTION STATEMENT A**

Approved for public release  
Distribution Unlimited

86 12 17 086

12

OFFICE OF NAVAL RESEARCH  
CONTRACT NO. N00014-81-K-0229  
PROJECT NO. 384-306

M. A. Breazeale, Principal Investigator

THE ULTRASONIC MEASUREMENT OF ELASTIC  
CONSTANTS OF CUBIC CRYSTALS

by

Madhu Puri

Ultrasonics Laboratory  
Department of Physics  
The University of Tennessee  
Knoxville, Tennessee 37996-1200

December 1986

IC  
ELECTE  
DEC 18 1986

Distribution of This Document is Unlimited

Unclassified

SECURITY CLASSIFICATION OF THIS PAGE (When Data Entered)

REPORT DOCUMENTATION PAGE		READ INSTRUCTIONS BEFORE COMPLETING FORM
1. REPORT NUMBER Technical Report No. 25	2. GOVT ACCESSION NO.	3. RECIPIENT'S CATALOG NUMBER
4. TITLE (and Subtitle) The Ultrasonic Measurement of Elastic Constants of Cubic Crystals		5. TYPE OF REPORT & PERIOD COVERED Interim
		6. PERFORMING ORG. REPORT NUMBER
7. AUTHOR(s) Madhu Puri		8. CONTRACT OR GRANT NUMBER(s) N00014-81-K-0229
9. PERFORMING ORGANIZATION NAME AND ADDRESS Department of Physics University of Tennessee Knoxville, TN 37996-1200		10. PROGRAM ELEMENT, PROJECT, TASK AREA & WORK UNIT NUMBERS 61153N; RR011-08-01; NR 384-306
11. CONTROLLING OFFICE NAME AND ADDRESS Office of Naval Research, Code 1112 Department of the Navy Arlington, VA 22217		12. REPORT DATE December 1986
		13. NUMBER OF PAGES 78
14. MONITORING AGENCY NAME & ADDRESS (if different from Controlling Office)		15. SECURITY CLASS. (of this report) Unclassified
		15a. DECLASSIFICATION/DOWNGRADING SCHEDULE
16. DISTRIBUTION STATEMENT (of this Report) Approved for public release; distribution unlimited		
17. DISTRIBUTION STATEMENT (of the abstract entered in Block 20, if different from Report)		
18. SUPPLEMENTARY NOTES		
19. KEY WORDS (Continue on reverse side if necessary and identify by block number) elastic constants sound velocity measurement error propagation		
20. ABSTRACT (Continue on reverse side if necessary and identify by block number) To evaluate the combination of third-order elastic constants $K_3$ of cubic crystals, one needs very accurate values of the combination of second-order elastic constants $K_2$ . Often one can obtain numerical values of second-order elastic constants for the sample of interest from existing data. Due to the error propagation and the experimental uncertainties at the time of the original measurement, however, there may be uncertainties in the magnitude of $K_2$ . An alternative way to arrive at $K_2$ 's would be to measure them at the time		

Unclassified

SECURITY CLASSIFICATION OF THIS PAGE (When Data Entered)

Block 20 continued:

the  $K_3$  data are taken. This measurement is quite straightforward since  $K_2$ 's are directly related to the sound velocities, which can be measured. The extra time and effort spent in doing the latter would be justified by an increase in accuracy. The purpose of this thesis is to study these alternatives and compare error propagation in an effort to arrive at the most accurate values of  $K_2$ . The analysis in this thesis shows that the question originally posed does not have a unique answer for all samples under all conditions. One cannot decide a priori whether the reference values of  $C_{ij}$  should be used or whether one should measure the  $C_{ij}$  each time one measures  $C_{ijk}$ . The analysis given, however, suggests that one should use reference data rather than measuring each sample, if the reference data are as accurate as those of McSkimin. If such accurate data are not available, one has no choice. One must measure the  $K_2$  directly.

S/N 0102- LF- 014- 6601

Unclassified

SECURITY CLASSIFICATION OF THIS PAGE (When Data Entered)

OFFICE OF NAVAL RESEARCH  
CONTRACT NO. N00014-81-K-0229  
PROJECT NO. 384-306

THE ULTRASONIC MEASUREMENT OF ELASTIC CONSTANTS  
OF CUBIC CRYSTALS

by

Madhu Puri

TECHNICAL REPORT NO. 25

Ultrasonics Laboratory  
Department of Physics  
The University of Tennessee  
Knoxville, TN 37996-1200



December 1986

Accession For	
NTIS CRA&I	<input checked="checked" type="checkbox"/>
DTIC TAB	<input type="checkbox"/>
Unannounced	<input type="checkbox"/>
Justification	
By	
Distribution/	
Availability Codes	
Dist	Avail and/or Special
A-1	

Approved for public release; distribution unlimited. Reproduction in whole or part is permitted for any purpose of the United States Government.

## PREFACE

To evaluate the combination of third-order elastic constants  $K_3$  of cubic crystals, one needs very accurate values of the combination of second-order elastic constants  $K_2$ . Often one can obtain numerical values of second-order elastic constants for the sample of interest from existing data. Due to the error propagation and the experimental uncertainties at the time of the original measurement, however, there may be uncertainties in the magnitude of  $K_2$ . An alternative way to arrive at  $K_2$ 's would be to measure them at the time the  $K_3$  data are taken. This measurement is quite straightforward since  $K_2$ 's are directly related to the sound velocities, which can be measured. The extra time and effort spent in doing the latter would be justified by an increase in accuracy. The purpose of this thesis is to study these alternatives and compare error propagation in an effort to arrive at the most accurate way to evaluate  $K_2$ . The analysis in this thesis shows that the question originally posed does not have a unique answer for all samples under all conditions. One cannot decide a priori whether the reference values of  $C_{ij}$  should be used or whether one should measure the  $C_{ij}$  each time one measures  $C_{ijk}$ . The analysis given, however, suggests that one should use reference data rather than measuring each sample, if the reference data are as accurate as those of McSkimin. If such accurate data are not available, one has no choice. One must measure the  $K_2$  directly.

It is difficult to find a good way to express my appreciation to all those who, in one way or another, helped me in the course of my studies at The University of Tennessee, Knoxville. I wish, however, to thank first Prof. M. A. Breazeale who encouraged me to enter this program and without whose guidance, support, and above all patience and understanding, the study and writing of this thesis would not have been possible.

Additional thanks are due to my other committee members, Professors C. C. Shih and J. O. Thomson, for reading this manuscript.

A very special thanks is extended to Mrs. Maxine Martin who has worked laboriously and patiently in typing and putting together this thesis.

My studies at The University of Tennessee were financed in a most generous way by the United States Office of Naval Research as well as by the Department of Physics, The University of Tennessee.

I also wish to thank Prof. G. Du for his helpful, constructive criticism of this investigation.

Finally, the author would like to express her most sincere gratefulness to her husband Tribhuvan and adorable son Dhruv for their cooperation, love and support, without which this long sought goal could not have been achieved.

## TABLE OF CONTENTS

CHAPTER	PAGE
I. INTRODUCTION: GENERALIZED DEFINITION OF ELASTIC CONSTANTS . . . . .	1
II. THEORY OF ELASTIC WAVE PROPAGATION . . . . .	6
A. Relation Between Stress and Strain in an Anisotropic Solid (Generalized Hooke's Law) . . . .	6
B. Second-Order Elastic Constants of Cubic Crystals . . . . .	7
C. Relation Between $C_{ij}$ 's and Sound Velocity . . . . .	9
1. Wave Speeds in an Elastic Medium . . . . .	9
2. Wave Speeds Along Pure Mode Directions in Cubic Crystals . . . . .	11
a. [100] Direction . . . . .	13
b. [110] Direction . . . . .	14
c. [111] Direction . . . . .	15
D. Summary . . . . .	15
III. EXPERIMENTAL APPARATUS AND PROCEDURE . . . . .	19
A. Capacitive Receiver Assembly . . . . .	19
B. Samples . . . . .	22
IV. EXPERIMENTAL RESULTS AND DATA ANALYSIS . . . . .	26
A. Experimental Data . . . . .	26
B. Data Analysis . . . . .	34
1. Assumptions and Methodology . . . . .	35
a. Functional Relationship Between F and Q . . . . .	35
b. Evaluation of Intercept $\alpha$ and Slope $\beta$ . . . . .	39
2. Use of Data in Ordinary Least Squares Estimates of $\beta$ and Velocities . . . . .	41
a. Computer Program . . . . .	41
b. Velocities in Germanium . . . . .	42
3. Comparison of Results with Reference Values .	45
a. Evaluation of Scatter of Data Around the Mean . . . . .	45
b. Comparison of Our Mean Value of Velocity with Values Given by McSkimin . . . . .	46
4. Error Propagation . . . . .	52
a. Error Propagation in the Present Experiment . . . . .	52

CHAPTER	PAGE
b. Error Propagation in Use of Reference Values of $C_{ij}$ . . . . .	54
5. Correction of Systematic Error . . . . .	56
V. SUMMARY . . . . .	61
REFERENCES . . . . .	62
APPENDIXES . . . . .	64
A. THEORY OF PULSE SUPERPOSITION TECHNIQUE . . . . .	65
B. COMPUTER PROGRAM FOR COMPUTING VELOCITY . . . . .	73

# LIST OF TABLES

TABLE	PAGE
1.1. $K_2$ and $K_3$ for [100], [110], and [111] Directions . . . . .	4
2.1. Expressions for Velocities and $K_2$ 's in a Cubic Crystal .	16
2.2. Combination of Second-Order Elastic Constants . . . . .	18
4.1. Sample Densities and Lengths . . . . .	27
4.2. Data for Ge[100] . . . . .	28
4.3. Data for Ge[110] . . . . .	29
4.4. Data for Ge[111] . . . . .	30
4.5. Estimated Regression Lines for Ge[100], Ge[110], and Ge[111] . . . . .	43
4.6. Estimated Velocity in Present Experiment and Velocity Reported by McSkimin . . . . .	44
4.7. Comparison of Velocities in Present Experiment with Those of McSkimin . . . . .	50
4.8. Propagated Error ( $\delta v/v$ ) in Present Experiment . . . . .	55
4.9. Propagated Error ( $\delta v/v$ ) from Standard Sources . . . . .	57
4.10. Corrected Estimates on Velocity in Present Experiment and Velocity Reported by McSkimin . . . . .	58
4.11. Comparison of Corrected Velocities in Present Experiment with Those of McSkimin . . . . .	59

## LIST OF FIGURES

FIGURE	PAGE
2.1. Principal Planes [100], [110], and [111] of a Cubic Crystal . . . . .	12
3.1. Block Diagram for the Velocity Measurements Using the Pulse Overlap Technique . . . . .	20
3.2. The Room Temperature Apparatus . . . . .	21
3.3. Dimensions of Samples Ge[100], Ge[110], and Ge[111] . . . . .	
4.1. Scatter Diagram of F vs. Q for Ge[100] . . . . .	31
4.2. Scatter Diagram of F vs. Q for Ge[110] . . . . .	32
4.3. Scatter Diagram of F vs. Q for Ge[111] . . . . .	33
4.4. Schematic Representation of Population Line $E(F) = \alpha + \beta Q$ and Sample Line $\hat{F} = \hat{\alpha} + \hat{\beta}Q$ . . . . .	40
4.5. Distribution of $f\left(\frac{\hat{\beta} - \beta_{111}}{S_{\hat{\beta}}}\right)$ . . . . .	48
A.1. Cross Sectional View of the Room Temperature Apparatus . . . . .	66
A.2. (a) A Typical Interference Pattern Obtained with the Pulse Overlap Technique; (b) and (c) Show the Separate Pulse Trains which Interfere to Give the Pattern of (a) . . . . .	67
A.3. Distances Travelled by Two Pulses after Undergoing Two Reflections at the Boundaries of the Sample . . . . .	69

## CHAPTER I

### INTRODUCTION: GENERALIZED DEFINITION OF ELASTIC CONSTANTS

The application of a time varying force on a solid material causes a deformation of the solid and gives rise to stress waves. To explain the behavior of a material upon application of stress, several general relations between stress applied and the resulting strain have been studied. One such relation was put forward by Hooke, according to which, for a linear elastic medium the stress applied to a material is proportional to the resulting strain, where the coefficient of proportionality is a constant independent of stress, strain and their time derivatives. Although Hooke's law generalized to anisotropic media is quite appropriate for description of many phenomena, it fails totally to explain nonlinear phenomena. Thus, a more general approach is required. Such a generalized approach was made by Murnaghan (1951) who started from the definition of the energy of a small volume subjected to a homogeneous strain. This approach later was applied to crystals of cubic symmetry by Holt and Ford (1967).

If  $\phi_0$  is the internal energy of a unit mass of material in an undeformed state, i.e., energy of the solid in equilibrium, then for small deformations we can expand the strain energy in a series

$$\phi = \phi_0 + \phi_1 + \phi_2 + \phi_3 + \dots \quad (1.1)$$

where  $\phi_1$  is the first-order perturbation term, etc. In terms of elastic moduli one can write the same expansion:

$$\begin{aligned} \phi = & \phi_0 + \frac{1}{1!} C_{ij} \eta_{ij} + \frac{1}{2!} C_{ijkl} \eta_{ij} \eta_{kl} \\ & + \frac{1}{3!} C_{ijklmn} \eta_{ij} \eta_{kl} \eta_{mn} + \dots \end{aligned} \quad (1.2)$$

where there is a summation over repeated indices which take successive values of 1, 2, and 3, and where  $C_{ij}$ 's are the elastic constants and  $\eta_{ij}$  are the components of a strain tensor. The first term on the right-hand side of Eq. (1.2),  $\phi_0$ , is independent of strain and therefore can be set equal to zero without loss of generality. The second term,  $\phi_1$ , is also set equal to zero, as it corresponds to displacement without deformation. Equation (1.2) then reduces to:

$$\phi = \frac{1}{2!} C_{ijkl} \eta_{ij} \eta_{kl} + \frac{1}{3!} C_{ijklmn} \eta_{ij} \eta_{kl} \eta_{mn} + \dots \quad (1.3)$$

where  $C_{ijkl}$  are the second-order elastic constants and  $C_{ijklmn}$  are the third-order elastic constants.

The expansion of strain energy in terms of strains can be substituted into Lagrange's equation to obtain a completely general wave equation capable of describing both linear and nonlinear wave phenomena in solids of any crystalline symmetry. Such an equation has been derived and has been specialized to cubic symmetry. For longitudinal waves along the principal directions in a cubic crystal the equation takes the form

$$\rho_0 \frac{\partial^2 u}{\partial t^2} = K_2 \frac{\partial^2 u}{\partial a^2} + 3K_2 + K_3 \frac{\partial^2 u}{\partial a^2} \frac{\partial u}{\partial a} \quad (1.4)$$

where the symbol  $K_2$  stands for linear combinations of second-order elastic constants and  $K_3$  stands for linear combinations of third-order elastic constants as shown in Table 1.1. The solution to the nonlinear wave equation is as follows:

$$u = A_1 \sin(ka - \omega t) - \left( \frac{3K_2 + K_3}{8K_2} \right) k^2 A_1^2 a \cos 2(ka - \omega t) + \dots \quad (1.5)$$

This solution shows that in a nonlinear solid the propagation of an initially sinusoidal wave generates a second harmonic whose amplitude is a linear function of propagation distance  $a$  and is proportional to the combination of elastic constants  $\frac{3K_2 + K_3}{K_2}$ . This combination often is called the nonlinearity parameter. Measurement of the amplitude of the second harmonic generated as a longitudinal ultrasonic wave propagates along the symmetry directions in cubic crystals has led to values of the third-order elastic constants of copper, germanium, silicon,  $KZnF_3$ ,  $SrTiO_3$ , and  $CsCdF_3$ , between room temperature and 77 °K, or even 3 °K.

But in the course of evaluating the third-order elastic constant,  $K_3$ , the experimenter must obtain values of the second-order elastic constants  $K_2$ , and the accuracy of the  $K_3$  is directly dependent upon the accuracy of  $K_2$ .

Since the second-order elastic constants of a number of crystals have been measured, it often is possible to obtain numerical values for the sample of interest from existing data. But the uncertainties in the magnitude of  $K_2$  depend upon error propagation as well as upon the experimental uncertainties at the time of the original measurement.

Table 1.1.  $K_2$  and  $K_3$  for [100], [110], and [111] Directions

Direction of Wave Propagation	$K_2$	$K_3$
[100]	$c_{11}$	$c_{111}$
[110]	$\frac{1}{2}(c_{11} + c_{12} + 2c_{44})$	$\frac{1}{4}(c_{111} + 3c_{112} + 12c_{166})$
[111]	$\frac{1}{3}(c_{11} + 2c_{12} + 4c_{44})$	$\frac{1}{9}(c_{111} + 6c_{112} + 12c_{144})$ $+ 24c_{166} + 2c_{123}$ $+ 16c_{456})$

An alternative way to arrive at expressions for  $K_2$  would be to measure them at the time the  $K_3$  data are taken. Since

$$K_2 = \rho v^2, \quad (1.6)$$

this measurement is quite direct—a measurement of the density of the material and of the velocity  $v$  of a longitudinal wave along the direction for which  $K_2$  is defined. An advantage of this procedure is that  $K_2$  data are taken on the same sample as the  $K_3$  data. But one disadvantage is that such a measurement would essentially double the time spent in measuring the third-order elastic constants as a function of temperature. Since such measurements typically require an uninterrupted period of at least 36 hours, such an increase in time would be justified only by an obvious increase in accuracy of the data.

The purpose of the present thesis is to evaluate the alternatives by comparing error propagation. To do this, measurements were made of the velocity of propagation in the three principal directions in germanium, a cubic crystal.

The data are subjected to a detailed error analysis and the results are compared with the errors propagated when the data of McSkimin (1963) are used to calculate velocities of longitudinal ultrasonic waves in germanium. The comparison is made more significant by the fact that the sample actually used by McSkimin was available for the measurements reported in this thesis.

## CHAPTER II

### THEORY OF ELASTIC WAVE PROPAGATION

The evaluation of the second-order elastic constants from data on the velocity of an ultrasonic wave in a cubic solid requires the derivation of the wave equation from the basic definitions. The basic definition of strain energy (Eq. 1.3) is general enough to allow a description of nonlinear phenomena; however, for purposes of deriving the linear form of the wave equation to be used throughout the remainder of this thesis, the strain energy can be approximated by including only the first set of terms. Since these terms contain second powers of the strain, the coefficients are known as second-order elastic constants. Truncation of the strain energy expansion in this way also allows one to make a definition of Hooke's law generalized to anisotropic media. Although the generalized Hooke's law has limited value since its very definition prohibits the consideration of third-order elastic constants, it still is used in engineering applications often enough to justify its consideration in this thesis.

#### A. RELATION BETWEEN STRESS AND STRAIN IN AN ANISOTROPIC SOLID (GENERALIZED HOOKE'S LAW)

To derive Hooke's law generalized to anisotropic media it is adequate to retain only the second power terms in the strain energy. Equation (1.3) thus becomes

$$\phi = \frac{1}{2} C_{ijkl} \eta_{ij} \eta_{kl} . \quad (2.1)$$

Now, consider the work done when a strain  $\eta_{ij}$  results from a stress  $\sigma_{ij}$ . The work  $E$  done by the stress in causing the strain is

$$E = \frac{1}{2} \sigma_{ij} \eta_{ij} . \quad (2.2)$$

Equating the work done to the strain energy results in

$$\sigma_{ij} = C_{ijkl} \eta_{kl} \quad (2.3)$$

This is known as the generalized Hooke's law for an anisotropic medium. In this form it can be used to describe a medium of any crystalline symmetry in the linear approximation.

#### B. SECOND-ORDER ELASTIC CONSTANTS OF CUBIC CRYSTALS

From Eq. (2.3) it appears that there must be  $3^4 = 81$  elastic constants  $C_{ijkl}$ . The total number of independent constants, however, is reduced by lattice symmetries. When the stress tensor  $\sigma_{ij}$  and the strain tensor  $\eta_{kl}$  are symmetric (i.e.,  $\sigma_{ij} = \sigma_{ji}$  and  $\eta_{kl} = \eta_{lk}$ ), the number of independent second-order constants reduces to  $6^2 = 36$ . This reduction is done easily by reindexing the stress and strain components according to Voigt rotation as follows:

$$\begin{aligned}
 \sigma_1 &= \sigma_{11} & , & & \sigma_4 &= \sigma_{23} = \sigma_{32} \\
 \sigma_2 &= \sigma_{22} & , & & \sigma_5 &= \sigma_{31} = \sigma_{13} \\
 \sigma_3 &= \sigma_{33} & , & & \sigma_6 &= \sigma_{12} = \sigma_{21}
 \end{aligned}$$

and

(2.8)

$$\begin{aligned}
 \eta_1 &= \eta_{11} & , & & \eta_4 &= \eta_{23} = \eta_{32} \\
 \eta_2 &= \eta_{22} & , & & \eta_5 &= \eta_{31} = \eta_{13} \\
 \eta_3 &= \eta_{33} & , & & \eta_6 &= \eta_{12} = \eta_{21}
 \end{aligned}$$

With this notation the linear relation between stress and strain is written as

$$\sigma_\alpha = C_{\alpha\beta} \eta_\beta \quad (\alpha, \beta = 1, 2, 3, 4, 5, 6) \quad (2.9)$$

where  $C_{\alpha\beta}$  are constants and the range of summation now is up to 6 for the indices  $\alpha$  and  $\beta$ . The elastic constants  $C_{\alpha\beta}$  and  $C_{ijkl}$  are related. Some examples of how these are related are shown below:

$$\begin{aligned}
 C_{11} &= C_{1111} \\
 C_{12} &= C_{1122} \\
 C_{14} &= 2C_{1123} = 2C_{1132} .
 \end{aligned} \quad (2.10)$$

We observe that  $C_{ijkl} = C_{jikr}$  and  $C_{ijkr} = C_{ijrk}$ . This implies that there are only six combinations for the first pair of indices and six of the second pair. Thus, for a cubic symmetry since,

$$C_{11} = C_{22} = C_{33}$$

$$C_{12} = C_{21} = C_{13} = C_{31} = C_{23} = C_{32}$$

$$C_{44} = C_{55} = C_{66}$$

the total number of independent elastic constants reduces to three, viz.  $C_{11}$ ,  $C_{12}$  and  $C_{44}$ .

### C. RELATION BETWEEN $C_{ij}$ 'S AND SOUND VELOCITY

#### 1. Wave Speeds in an Elastic Medium

The linear equation of motion for a wave through an elastic medium can be derived by using the strain energy Eq. (2.1) in Lagrange's equation. As given by Green (1973) it is:

$$\rho \ddot{u}_i = C_{ijkl} \frac{\partial^2 u_k}{\partial x_l \partial x_j} \quad (2.11)$$

where  $C_{ijkl}$  are the second-order elastic constants,  $u_i$  is the displacement at a time  $t$ , and  $\rho$  is the mass density of the homogeneous medium. In the principal directions [100], [110], and [111] in a cubic lattice the three equations represented in Eq. (2.11) are uncoupled, and to derive a relation between wave speeds and  $C_{ij}$ 's in these directions we assume a solution to Eq. (2.11) of the form:

$$u_i(x_k, t) = A_0 \alpha_i \exp i(\omega t - k_m x_m) \quad (2.12)$$

where  $A_0$  is the amplitude of the wave,  $\alpha_i$  are the direction cosines of the displacement vector,  $k_m$  is the wave vector given by

$$k_m = k_{\ell_m} = \left(\frac{2\pi}{\lambda}\right) \ell_m, \quad (2.13)$$

where  $k$  is the wave number,  $\ell_m$  ( $= \ell, m, n$ ) are the direction cosines of the normal to the plane wave, and  $\lambda$  is the wavelength. Substituting Eq. (2.12) into Eq. (2.11) and using Eq. (2.13) gives a set of equations of the form

$$[C_{ijk\ell} \cdot \ell_\ell \ell_j - \rho v^2 \delta_{ik}] u_k = 0 \quad (2.14)$$

where  $v$ , the speed of propagation of the wave, is given by

$$v^2 = \omega^2 / k^2 \quad (2.15)$$

and  $u_i = \ell_i u_k$ . For a nontrivial solution of Eq. (2.14) to exist, the determinant of the coefficient must vanish. Thus,

$$|C_{ijk\ell} \ell_\ell \ell_j - \rho v^2 \delta_{ik}| = 0. \quad (2.16)$$

For simplicity, let  $C_{ijk\ell} \ell_\ell \ell_j = \lambda_{ik}$ ; then (2.16) reduces to

$$|\lambda_{ik} - \rho v^2 \delta_{ik}| = 0. \quad (2.17)$$

Equation (2.17) is an eigenvalue problem of the form

$$\left| \begin{pmatrix} \lambda_{11} & \lambda_{12} & \lambda_{13} \\ \lambda_{21} & \lambda_{22} & \lambda_{23} \\ \lambda_{31} & \lambda_{32} & \lambda_{33} \end{pmatrix} - \rho v^2 \begin{pmatrix} 1 & 0 & 0 \\ 0 & 1 & 0 \\ 0 & 0 & 1 \end{pmatrix} \right| = 0 \quad (2.18)$$

whose solution gives the wave speeds. This determinant can be written in the form

$$\begin{vmatrix} \lambda_{11} - \rho v^2 & \lambda_{12} & \lambda_{13} \\ \lambda_{21} & \lambda_{22} - \rho v^2 & \lambda_{23} \\ \lambda_{31} & \lambda_{32} & \lambda_{33} - \rho v^2 \end{vmatrix} = 0. \quad (2.19)$$

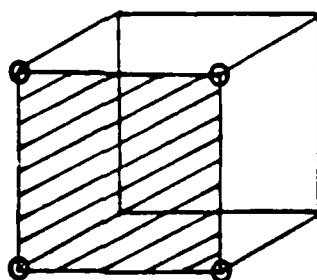
The fact that this is a  $3 \times 3$  determinant indicates that there are three solutions; i.e., there are three independent plane waves, each having polarization in one of the three orthogonal directions. The speeds of these waves are the eigenvalues. To determine the eigenvectors we define the direction cosines  $\alpha, \beta, \gamma$  of the particle displacements. They are obtained by writing Eq. (2.16) in the form:

$$\begin{pmatrix} \lambda_{11} & \lambda_{12} & \lambda_{13} \\ \lambda_{21} & \lambda_{22} & \lambda_{23} \\ \lambda_{31} & \lambda_{32} & \lambda_{33} \end{pmatrix} \begin{pmatrix} \alpha \\ \beta \\ \gamma \end{pmatrix} = \rho v^2 \begin{pmatrix} 1 & 0 & 0 \\ 0 & 1 & 0 \\ 0 & 0 & 1 \end{pmatrix} \begin{pmatrix} \alpha \\ \beta \\ \gamma \end{pmatrix} \quad (2.20)$$

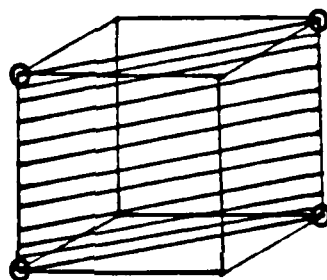
where we have used  $\delta_{ik} = \begin{pmatrix} 1 & 0 & 0 \\ 0 & 1 & 0 \\ 0 & 0 & 1 \end{pmatrix}$ . The solution of this equation gives the eigenvectors. To repeat, the solution of the eigenvalue problem (2.17) for eigenvalues and eigenvectors gives information about the magnitude and direction of the speed of propagation of the three possible plane waves through a crystal. It is specialized to the pure mode directions in cubic crystals in the next section.

## 2. Wave Speeds Along Pure Mode Directions in Cubic Crystals

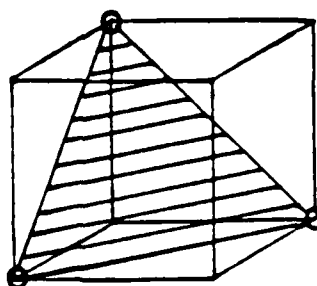
The three principal directions in cubic crystals are shown in Figure 2.1. In each of these directions three pure mode elastic waves (one longitudinal and two transverse) may propagate, while in all the other directions waves may be coupled. We now study the behavior of



**[100]**



**[110]**



**[111]**

Figure 2.1. Principal planes [100], [110], and [111] of a cubic crystal.

the elastic waves along the pure mode directions of cubic crystals and derive relations between sound velocities and  $C_{ij}$ 's.

a. [100] Direction

For the [100] plane ~~the~~ direction cosines of the plane wave normal are  $l = 1$ ,  $m = 0$ ,  $n = 0$ . For this direction,

$$\lambda_{11} = C_{11}$$

$$\lambda_{12} = \lambda_{13} = \lambda_{23} = \lambda_{21} = \lambda_{31} = \lambda_{32} = 0$$

$$\lambda_{22} = \lambda_{33} = C_{44}$$

Substitution of these values into (2.17) and simplification leads to:

$$(C_{11} - \rho v^2)(C_{44} - \rho v^2)(C_{44} - \rho v^2) = 0$$

whose three solutions give the magnitude of the three wave speeds:

$$\begin{aligned} v_1 &= \left( \frac{C_{11}}{\rho} \right)^{1/2} && \text{(longitudinal)} \\ v_2 &= v_3 = \left( \frac{C_{44}}{\rho} \right)^{1/2} && \text{(transverse)} \end{aligned} \tag{2.22}$$

The direction of propagation of these three waves is obtained by evaluating the eigenvectors  $\alpha$ ,  $\beta$ ,  $\gamma$  from Eq. (2.21) for each of the speeds  $v_1$ ,  $v_2$ , and  $v_3$ . For velocity  $v_1$ , we find  $\alpha = 1$ ,  $\beta = 0$ , and  $\gamma = 0$ . A comparison of  $\alpha$ ,  $\beta$ ,  $\gamma$  with  $l$ ,  $m$ ,  $n$  shows that the direction cosines of the particle displacement are identical to the direction cosines of the plane wave normal; i.e., speed  $v_1$  corresponds to a pure mode longitudinal wave. Similar calculations for  $\alpha$ ,  $\beta$ ,  $\gamma$  for speeds  $v_2$  and  $v_3$  show that  $v_2$  and  $v_3$  correspond to pure mode transverse waves and that  $|v_2| = |v_3|$ ; i.e., the two transverse waves propagate at the same speed. This means that the speed of a transverse wave propagating along the [100] direction is independent of polarization.

b. [110] Direction

For the [110] plane, the direction cosines of the wave normal are  $\ell = 1/\sqrt{2}$ ,  $m = 1/\sqrt{2}$ ,  $n = 0$ . For this direction,

$$\begin{aligned}\lambda_{11} &= \lambda_{22} = \frac{1}{2} (C_{11} + C_{44}) \\ \lambda_{12} &= \lambda_{21} = \frac{1}{2} (C_{12} + C_{44}) \\ \lambda_{13} &= \lambda_{23} = \lambda_{31} = \lambda_{32} = 0 \\ \lambda_{33} &= C_{44} .\end{aligned}\tag{2.23}$$

Substitution of these values into Eq. (2.17) and simplification gives:

$$\left( \frac{1}{2}(C_{11} - C_{12}) - \rho v^2 \right) \left( \frac{1}{2}(C_{11} + C_{12} + 2C_{44}) - \rho v^2 \right) \left( C_{44} - \rho v^2 \right) = 0 .\tag{2.24}$$

Solution of Eq. (2.24) gives the magnitude of the three wave speeds:

$$\begin{aligned}v_1 &= \{(C_{11} + C_{12} + 2C_{44})/2\rho\}^{1/2} \\ v_2 &= \{(C_{11} - C_{12})/2\rho\}^{1/2} \\ v_3 &= \{C_{44}/\rho\}^{1/2}\end{aligned}\tag{2.25}$$

The direction of propagation of these three waves is obtained by evaluating the eigenvectors  $\alpha$ ,  $\beta$ , and  $\gamma$  from (2.21) for each of the speeds  $v_1$ ,  $v_2$ , and  $v_3$ . Note that in this case  $v_2 \neq v_3$ . For the speed  $v_1$  we find that  $\alpha = 1/\sqrt{2}$ ,  $\beta = 1/\sqrt{2}$ ,  $\gamma = 0$ . A comparison of  $\alpha$ ,  $\beta$ , and  $\gamma$  with  $\ell$ ,  $m$ , and  $n$  shows that the two sets are identical, so  $v_1$  is a pure mode longitudinal wave. Similar calculations of  $\alpha$ ,  $\beta$ ,  $\gamma$  for the speeds  $v_2$  and  $v_3$ , and comparison with  $\ell$ ,  $m$ , and  $n$  shows that they are pure mode transverse waves.

c. [111] Direction

The direction cosines of the wave normal in the [111] direction are  $\ell = m = n = 1/\sqrt{3}$ . For this direction,

$$\begin{aligned}\lambda_{11} &= \lambda_{22} = \lambda_{33} = \frac{1}{2} (C_{11} + 2C_{44}) \\ \lambda_{12} &= \lambda_{13} = \lambda_{23} = \lambda_{21} = \lambda_{31} = \lambda_{32} = \frac{1}{3} (C_{12} + C_{44}) .\end{aligned}\tag{2.26}$$

Using Eqs. (2.26) and (2.17), the magnitudes of the three wave speeds are given by

$$\begin{aligned}v_1 &= \left( \frac{C_{11} + 2C_{12} + 4C_{44}}{3\rho} \right)^{1/2} \\ v_2 &= v_3 = \left( \frac{C_{11} - C_{12} + C_{44}}{3\rho} \right)^{1/2}\end{aligned}\tag{2.27}$$

Again, evaluating the eigenvectors for each of the speeds  $v_1$ ,  $v_2$ , and  $v_3$  shows that for  $v_1$   $\alpha = \beta = \gamma = 1/\sqrt{3}$ .

Comparison of  $\alpha$ ,  $\beta$ , and  $\gamma$  with  $\ell$ ,  $m$ , and  $n$  shows that  $v_1$  is longitudinal. Similar comparisons show that  $v_2$  and  $v_3$  are transverse and equal in magnitude.

#### D. SUMMARY

The relationship between sound velocity and  $C_{ij}$ 's has been derived for the three principal directions [100], [110], and [111] in a cubic crystal. The results are summarized in Table 2.1 where it is clear that in the [100] and [111] directions the two transverse waves travel at the same speed, but in the [110] direction their speeds are

Table 2.1. Expressions for Velocities and  $K_2$ 's in a Cubic Crystal

Direction	$(\ell, m, n)^a$	$(\alpha, \beta, \gamma)^b$	$\begin{matrix} v_1 \\ v_2 \\ v_3 \end{matrix}$	Mode of Propagation	$K_2$
[100]	1, 0, 0	1, 0, 0	$v_1 = \left[ \frac{C_{11}}{\rho} \right]^{1/2}$	Longitudinal	$C_{11}$
			$v_2 = v_3 = \left[ \frac{C_{44}}{\rho} \right]^{1/2}$	Transverse	
[110]	$\frac{1}{\sqrt{2}}, \frac{1}{\sqrt{2}}, 0$	$\frac{1}{\sqrt{2}}, \frac{1}{\sqrt{2}}, 0$	$v_1 = \left[ \frac{C_{11} + C_{12} + 2C_{44}}{2\rho} \right]^{1/2}$	Longitudinal	$\frac{C_{11} + C_{12} + 2C_{44}}{2}$
			$v_2 = \left[ \frac{C_{11} - C_{12}}{2\rho} \right]^{1/2}$	Transverse	
			$v_3 = \left[ \frac{C_{44}}{\rho} \right]^{1/2}$	Transverse	
[111]	$\frac{1}{\sqrt{3}}, \frac{1}{\sqrt{3}}, \frac{1}{\sqrt{3}}$	$\frac{1}{\sqrt{3}}, \frac{1}{\sqrt{3}}, \frac{1}{\sqrt{3}}$	$v_1 = \left[ \frac{C_{11} + 2C_{12} + 4C_{44}}{3\rho} \right]^{1/2}$	Longitudinal	$\frac{C_{11} + 2C_{12} + 4C_{44}}{3}$
			$v_2 = v_3 = \left[ \frac{C_{11} - C_{12} + C_{44}}{3\rho} \right]^{1/2}$	Transverse	

<sup>a</sup>Direction cosines of plane wave normal.<sup>b</sup>Direction cosines of particle displacements.

different. For the purposes of this thesis one is interested in the relationship between  $C_{ij}$ 's and sound velocity for longitudinal waves, as the relationship among the  $C_{ij}$ 's for longitudinal waves presented in Table 2.1 are identical with those labelled  $K_2$  in Table 1.1, p. 4. To emphasize this point the results for the longitudinal waves in the principal direction are repeated in Table 2.2. These are the relationships to be analyzed.

Table 2.2. Combination of Second-Order Elastic Constants

Direction of Propagation	$\frac{K_2}{\rho} = v_{\text{longitudinal}}^2$
[100]	$\frac{C_{11}}{\rho}$
[110]	$\frac{C_{11} + C_{12} + 2C_{44}}{2\rho}$
[111]	$\frac{C_{11} + 2C_{12} + 4C_{44}}{3\rho}$

## CHAPTER III

### EXPERIMENTAL APPARATUS AND PROCEDURE

The configuration used in the measurement of the velocity of sound and the related  $K_2$ 's in samples of germanium is shown in Figure 3.1. Electrical pulses modulated at 30 MHz are generated by the gated amplifier. They arrive at the transducer surface through the impedance matching network and cause the transducer to vibrate and generate a 30 MHz pulse of ultrasonic waves which propagate through the sample and are received by the capacitive receiver which converts them to an electrical signal which is amplified and displayed on an oscilloscope.

#### A. CAPACITIVE RECEIVER ASSEMBLY

Details of the capacitive receiver are given in Figure 3.2. The upper end of the receiver assembly consists of a copper electrode 1 cm in diameter surrounded by a grounded outer assembly that is insulated from the electrode by a Teflon ring. The electrode is spring-loaded to make contact with the quartz transducer surface. The electrical signal is fed to the quartz transducer through the spring.

At the lower end of the assembly is an electrode of 1 cm diameter placed on a fused silica optical flat. A grounded concentric copper ring in contact with the optically flat end of the sample provides an air gap between the electrode and the sample, a separation of the order of 10 microns. When the sample is placed in position, it

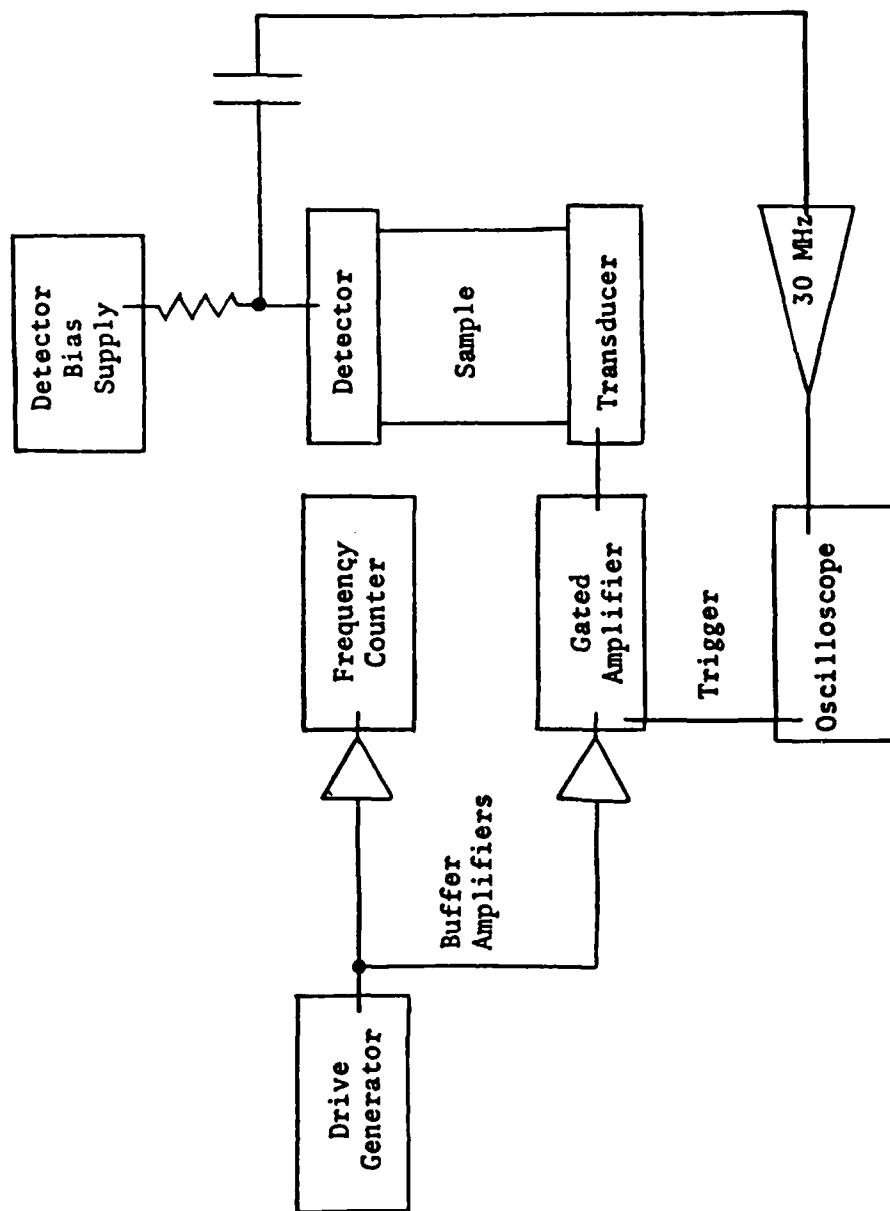


Figure 3.1. Block diagram for the velocity measurements using the pulse overlap technique.

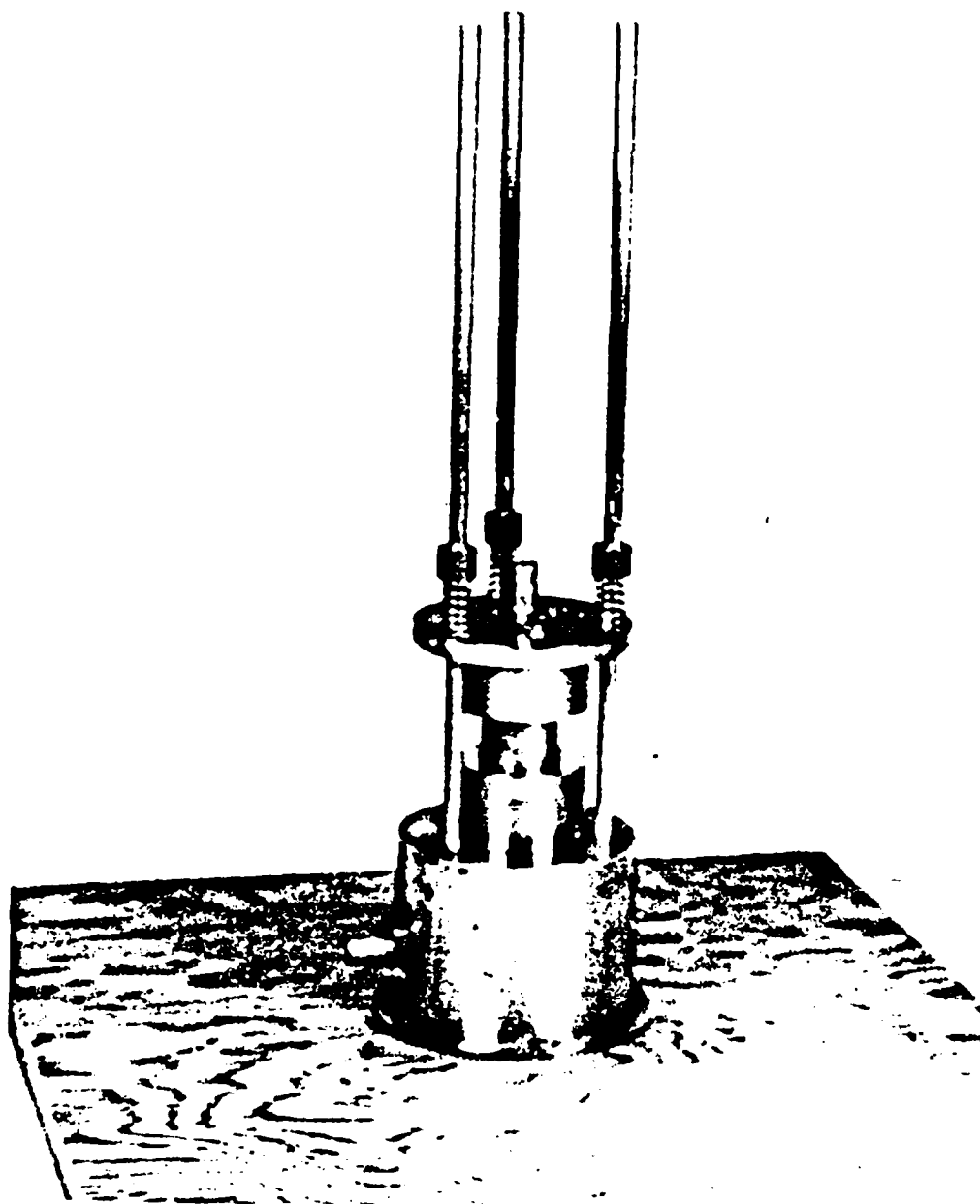


Figure 3.2. The room temperature apparatus.

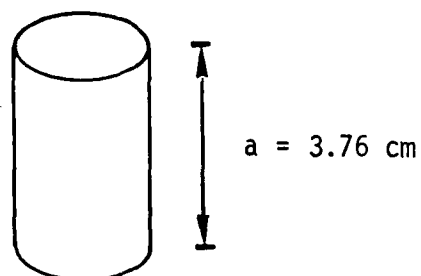
touches the outer ring. The optically flat sample face and the electrode surfaces form a parallel plate capacitor with air as dielectric, as shown schematically in Figure 3.2. The capacitance of the parallel plate capacitor may be evaluated from

$$C = \epsilon \cdot \frac{A}{d},$$

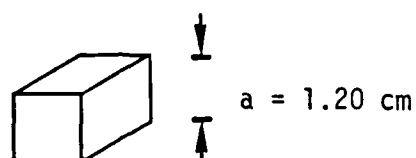
where  $A$  is the area of the plates and  $d$  is the spacing between the plates ( $5\mu$ - $10\mu$ ), since the fringing is negligible. The capacitance is found to be of the order of 60-120 pF for a spacing of  $d = 5$ -10 microns and for detector diameter = 0.92 cm.

## B. SAMPLES

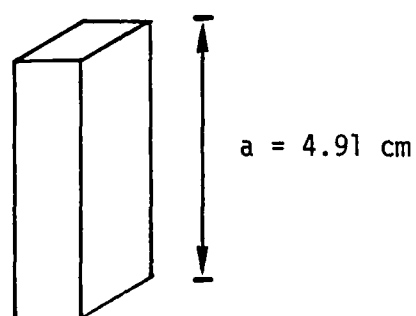
Measurement of the velocity of sound was made in the laboratory on several materials, but in the present thesis the focus is on samples of germanium single crystals. The lattice structure of germanium is cubic and there are three directions along which pure longitudinal ultrasonic waves propagate in cubic lattices:  $[100]$ ,  $[110]$ , and  $[111]$ . The samples allowed measurements to be made along these pure mode directions. They are sketched in Figure 3.3 with the dimensions indicated. The samples were first lapped to a flatness of half a wavelength of light. The importance of making the samples optically flat results from the plane wave assumption used in the theory of ultrasonic wave propagation. Since we used high frequency ( $\sim 30$  MHz), which corresponds to a wavelength of 0.17 mm for germanium, even a small variation in the surface can produce a significant phase shift and affect the accuracy of the experiment.



**A. Ge 100**



**B. Ge 110**



**C. Ge 111**

Figure 3.3. Dimensions of samples Ge[100], Ge[110], and Ge[111].

After the samples were lapped, they were washed thoroughly to remove any oil that might have impeded the adherence of a copper coating. The samples were placed in a vacuum of  $10^{-6}$  Torr and allowed to outgas for one hour. Then a  $100 \text{ \AA}$  coating of copper was sputtered onto the surface to serve as an electrode. After removal of the sample from the vacuum chamber, a quartz transducer was attached to one of the optically flat conducting surfaces by means of nonaqueous stopcock grease, then the sample was mounted in the measurement assembly.

The output of the cw oscillator (see Figure 3.1) was applied to the gated amplifier whose output was tested with an oscilloscope and applied through an impedance matching network across the quartz transducer attached to the sample surface. By adjustment of the impedance matching network, the pulsed oscillator-transducer system was tuned for maximum power transmitted to the quartz transducer whose resonant frequency was 30 MHz.

The 30 MHz pulsed ultrasonic wave generated by the transducer travels through the sample and is reflected between the sample surfaces. When it reaches the lower surface, it causes the sample surface to vibrate. As a result, the capacitance between the surface and electrode, as shown in Figure 3.2, changes periodically. This produces an alternating current which is amplified and observed on the oscilloscope. The gated amplifier is capable of generating a second pulse train (delayed in time with respect to the first pulse train). The two pulsed ultrasonic waves interfere and give rise to interference maxima and minima.

For a minimum, the path difference between the two pulses must contain an odd number of half-wavelengths; viz,

$$\text{Path difference} = (m + \frac{1}{2}) \lambda$$

where  $m = 0, 1, 2, \dots$ . In taking data an initial frequency in the range of the resonance frequency was chosen. Then a number of minima was counted as the frequency was increased, and the final frequency noted.

If the  $n$ th echo of one pulse train overlapped the  $m$ th echo of the second pulse train, the difference  $m - n = s$  is the quantity used in calculating the velocity.

Finally, the length  $L$  of the sample was measured with an accuracy of  $10^{-4}$  cm. The velocity of the ultrasound in the sample material was then determined using the expression:

$$v = \frac{2Ls \Delta F}{\Delta Q}$$

where

$L$  = the length of the sample;

$s = m - n$  ( $n$  is the echo number of some initial pulse and  $m$  is the echo number of some other pulse delayed in time with respect to the first pulse);

$\Delta F$  = frequency difference;

$\Delta Q$  = the number of interference minima.

## CHAPTER IV

### EXPERIMENTAL RESULTS AND DATA ANALYSIS

The error propagation in determining the  $K_2$ 's from expressions for  $C_{ij}$  can be evaluated directly from the data; however, in order to evaluate the relative magnitude of the propagated error and the error resulting from direct measurement of the  $K_2$ 's it was necessary to set up apparatus and measure the velocity of longitudinal waves in crystalline samples. The calculations given in Chapter II show that the expressions for the  $K_2$ 's are related to the measured velocities by  $K_2 = \rho v^2$ . This chapter describes the means by which experimental values of the longitudinal wave velocities were obtained.

#### A. EXPERIMENTAL DATA

The length and the density of the samples used in the present experiment, viz. Ge(100), Ge(110), and Ge(111), are given in Table 4.1. Three sets of data, using 30 MHz transducers were taken for the measurement of velocity of sound in the samples of germanium. For each set of data, a measurement of frequency  $F$  was taken for several values of the maxima  $Q$ . The data are presented in Tables 4.2, 4.3, and 4.4. Plots of  $F$  versus  $Q$  are shown for each of the samples in Figures 4.1, 4.2, and 4.3. These figures, usually called scatter diagrams, allow one to observe directly the scatter of the data resulting from statistical variations in the magnitudes of the measured quantities. Under ideal circumstances these variations would vanish and the data in each case

Table 4.1. Sample Densities and Lengths

Sample	Length (cm)	Density (gm/cm <sup>3</sup> )
Ge[100]	3.76	5.323
Ge[110]	1.20	5.323
Ge[111]	4.91	5.323

Table 4.2. Data for Ge[100]

S = 1			S = 1			S = 1		
Obs.	Q	F(MHz)	Obs.	Q	F(MHz)	Obs.	Q	F(MHz)
1	0	27.872	31	50	31.209	61	80	33.290
2	10	28.523	32	60	31.879	62	0	27.802
3	20	29.192	33	70	32.518	63	10	28.590
4	30	29.840	34	80	33.189	64	20	29.201
5	40	30.504	35	0	27.818	65	30	29.867
6	50	31.146	36	10	28.463	66	40	30.601
7	60	31.795	37	20	29.131	67	50	31.149
8	70	32.465	38	30	20.778	68	60	31.812
9	0	27.872	39	40	30.425	69	70	32.501
10	10	28.542	40	50	31.076	70	80	33.298
11	20	29.194	41	60	31.729	71	90	33.601
12	30	20.856	42	70	32.401	72	0	27.859
13	40	30.563	43	80	33.055	73	10	28.498
14	50	31.211	44	0	27.814	74	20	29.199
15	60	31.878	45	10	28.467	75	30	29.901
16	70	32.518	46	20	29.128	76	40	30.598
17	80	33.279	47	30	29.816	77	50	31.201
18	0	27.851	48	40	30.444	78	60	31.852
19	10	28.546	49	50	31.084	79	70	32.559
20	20	29.201	50	60	31.746	80	80	33.302
21	30	29.840	51	70	32.401	81	90	33.643
22	40	30.578	52	80	33.066			
23	50	31.102	53	0	27.862			
24	60	31.800	54	10	28.495			
25	70	32.468	55	20	29.179			
26	0	27.920	56	30	29.848			
27	10	28.594	57	40	30.509			
28	20	29.252	58	50	31.157			
29	30	29.911	59	60	31.843			
30	40	30.576	60	70	32.508			

Table 4.3. Data for Ge[110]

S = 2				S = 2				S = 2			
Obs.	Q	F (MHz)		Obs.	Q	F (MHz)		Obs.	Q	F (MHz)	
1	0	24.926		31	30	28.291		61	60	31.639	
2	10	26.079		32	40	29.443		62	63	32.029	
3	20	27.159		33	50	30.515		63	70	32.690	
4	30	28.276		34	60	31.662					
5	40	29.403		35	63	32.060					
6	50	30.508		36	70	32.707					
7	60	31.632		37	0	24.811					
8	63	32.015		38	10	26.055					
9	70	32.701		39	20	27.150					
10	0	24.940		40	30	28.195					
11	10	26.101		41	40	29.400					
12	20	27.160		42	50	30.403					
13	30	28.277		43	60	31.702					
14	40	29.409		44	63	32.019					
15	50	30.510		45	70	32.602					
16	60	31.641		46	0	24.820					
17	63	32.020		47	10	26.055					
18	70	32.705		48	20	27.150					
19	0	24.963		49	30	28.215					
20	10	26.091		50	40	29.382					
21	20	27.165		51	50	30.400					
22	30	28.279		52	60	31.645					
23	40	29.451		53	63	32.030					
24	50	30.590		54	70	32.700					
25	60	31.652		55	0	24.799					
26	63	32.019		56	10	26.069					
27	70	32.713		57	20	27.158					
28	0	24.935		58	30	28.227					
29	10	26.080		59	40	29.317					
30	20	27.169		60	50	30.391					

Table 4.4. Data for Ge[111]

Obs.	Q	F	Obs.	Q	F	Obs.	Q	F
1	0	25.689	37	20	26.835	73	70	29.865
2	10	26.266	38	30	27.402	74	80	30.430
3	20	26.836	39	40	27.993	75	90	30.998
4	30	27.403	40	50	28.553	76	100	31.581
5	40	27.988	41	60	29.126	77	110	32.146
6	50	28.557	42	70	29.700	78	120	32.717
7	60	29.128	43	80	30.269	79	130	33.303
8	70	29.700	44	90	30.833	80	140	33.811
9	80	30.272	45	100	31.397	81	0	25.792
10	90	30.832	46	110	31.989	82	10	26.373
11	100	31.399	47	120	32.547	83	20	26.943
12	110	31.983	48	130	33.140	84	30	27.497
13	120	32.546	49	140	33.712	85	40	28.068
14	130	33.133	50	150	34.246	86	50	28.652
15	140	33.687	51	0	25.863	87	60	29.228
16	150	34.266	52	10	26.428	88	70	29.801
17	160	34.752	53	20	26.992	89	80	30.376
18	0	25.684	54	30	27.568	90	90	30.938
19	10	26.266	55	40	28.144	91	100	31.503
20	20	26.832	56	50	28.714	92	110	32.085
21	30	27.400	57	60	29.302	93	120	32.673
22	40	27.974	58	70	29.865	94	130	33.235
23	50	28.530	59	80	30.429	95	140	33.801
24	60	29.124	60	90	30.995	96	0	25.792
25	70	29.685	61	100	31.564	97	10	26.318
26	80	30.268	62	110	32.150	98	20	26.889
27	90	30.833	63	120	32.714	99	30	27.481
28	100	31.398	64	130	33.296	100	40	28.036
29	110	31.979	65	140	33.817	101	50	28.610
30	120	32.554	66	0	25.863	102	60	29.183
31	130	33.105	67	10	26.425	103	70	29.779
32	140	33.701	68	20	26.996	104	80	30.318
33	150	34.261	69	30	27.568	105	90	30.886
34	160	34.752	70	40	28.155	106	100	31.452
35	0	25.684	71	50	28.744	107	110	32.043
36	10	26.266	72	60	29.301	108	120	32.625

PLOT OF  $F \cdot Q$       LEGEND: A = 1 OBS, B = 2 OBS, ETC.

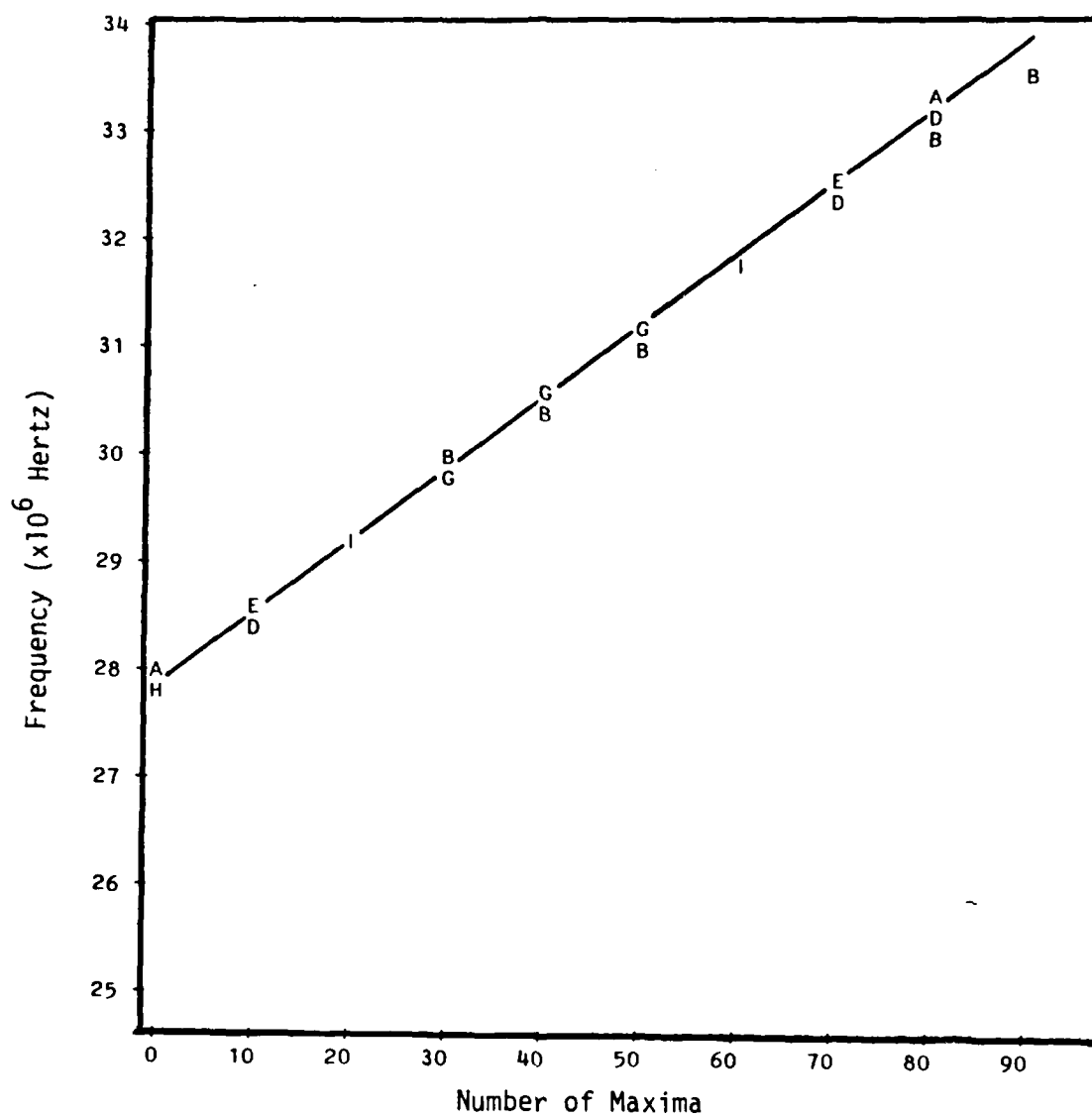


Figure 4.1. Scatter diagram of  $F$  vs.  $Q$  for Ge[100].

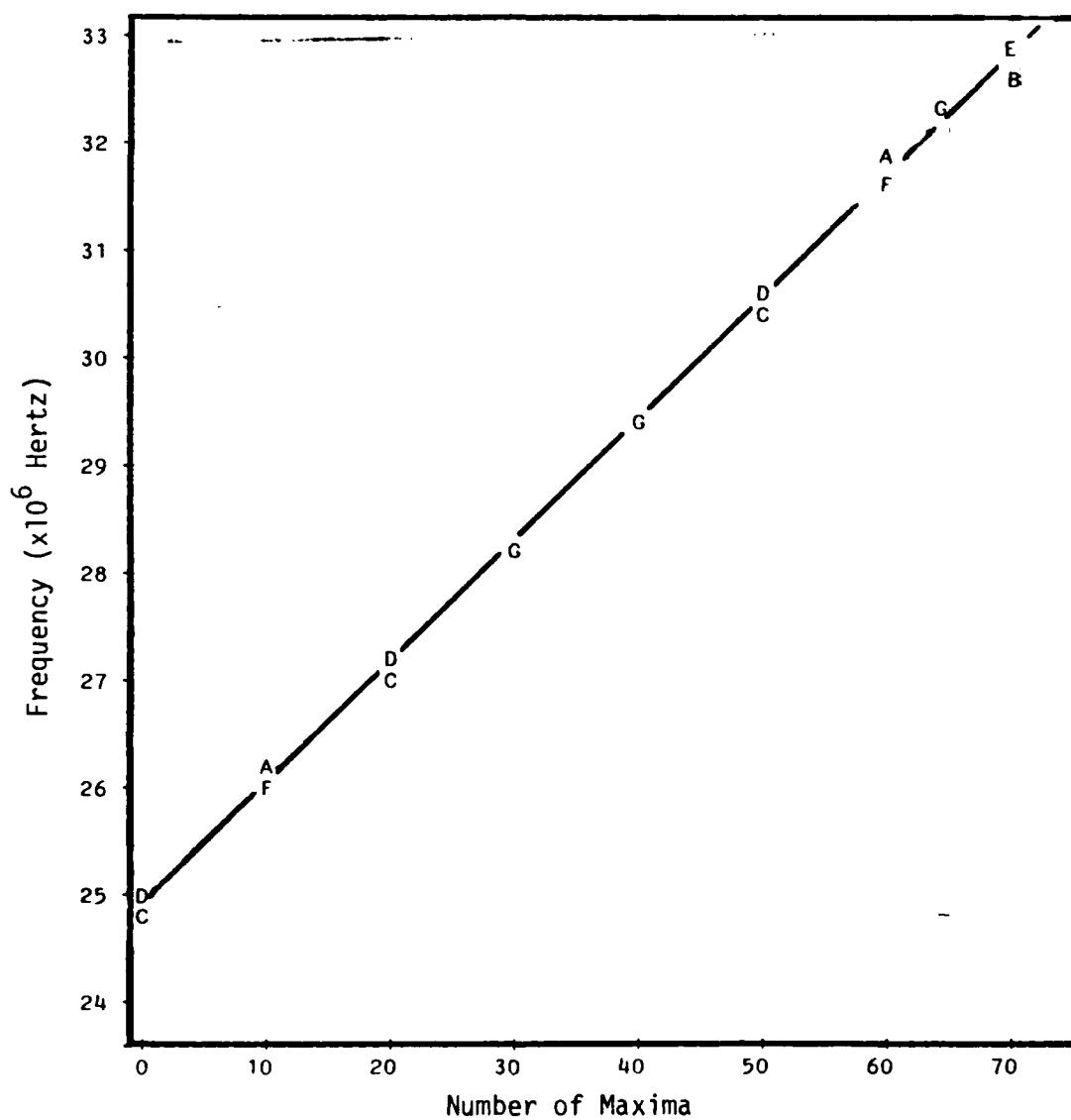
PLOT OF  $F \cdot Q$     LEGEND: A = 1 OBS, B = 2 OBS, ETC.

Figure 4.2. Scatter diagram of F vs. Q for Ge[110].

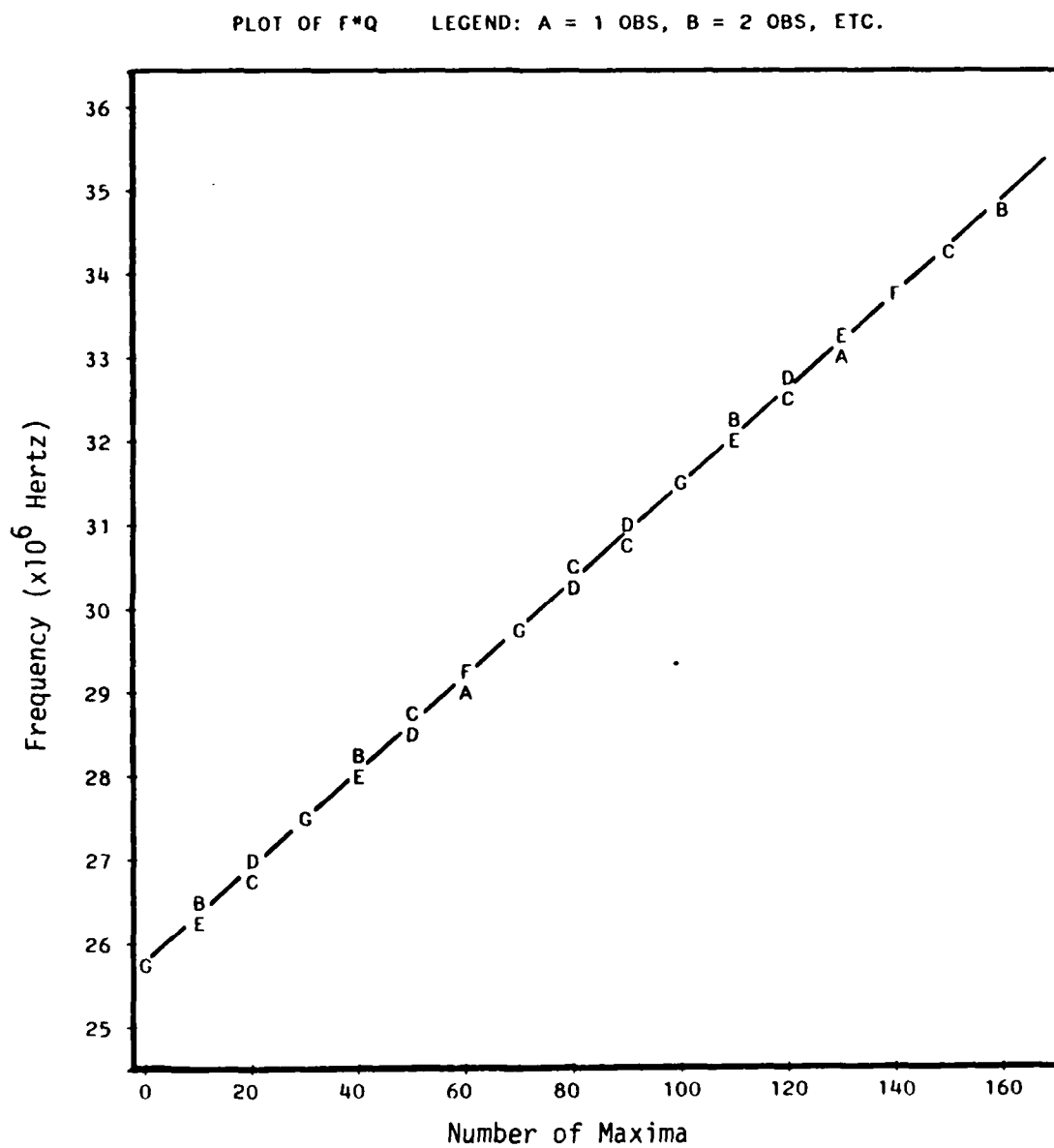


Figure 4.3. Scatter diagram of  $F$  vs.  $Q$  for Ge[111].

would define a single straight line whose slope in combination with  $L$  and  $s$  would give the exact value of the velocity in the corresponding direction. The purpose of the next section is to define the way one handles the actual data to arrive at the most probable straight line, one that is a very good approximation to the exact one.

## B. DATA ANALYSIS

To calculate the velocity of sound in the germanium crystal for various crystalline modes one uses the expression

$$v = 2 Ls \frac{\Delta F}{\Delta Q} \quad (4.1)$$

and the observations on  $L$ ,  $s$  ( $m$  and  $n$ ),  $F$ , and  $Q$  presented above. The observations on  $F$  and  $Q$  presented in the scatter diagrams (Figures 4.1, 4.2, 4.3) suggest that for any interval  $\Delta Q$  the corresponding interval  $\Delta F$  is not uniform for all values of  $Q$ . For example, if  $\Delta Q = Q_2 - Q_1$  and  $\Delta F = F_2 - F_1$ , then for a different  $\Delta Q = Q_4 - Q_3$  ( $= Q_2 - Q_1$ ),  $F_4 - F_3$  can be different from  $\Delta F = F_2 - F_1$ . This is because the data on  $F$  and  $Q$  in practice do not have an exact functional relationship as a result of systematic and random errors in the experiment. It therefore is important statistically to estimate the best value of  $\Delta F/\Delta Q$  from the data in order to predict the most probable value of the velocity  $v$ . This is the purpose of the present section which is divided into five parts.

The first part deals with the assumptions, relevant formulae, and methodology employed in the estimation of  $\Delta F/\Delta Q$ . In the second part, ordinary least squares estimates of the slope  $B = \Delta F/\Delta Q$  are

presented in the standard format and also in a table. Computations of velocity are then made and the results are shown in tabular form.

In the third part, the experimental results on velocity in the germanium crystals are compared with those obtained by McSkimin (1963). The propagation of errors in the present experiment and propagation of error in calculating velocity using standard values of second-order elastic constants are discussed in the fourth part. Lastly, in the fifth part are presented the conclusions.

### 1. Assumptions and Methodology

The method of ordinary least squares is used to estimate the most probable value of the slope  $\beta = \Delta F / \Delta Q$  from the data. But in order to do so it is essential to make the (unverifiable) assumption that the statistical distribution of  $F$  does not change from one set of observations to another. The evaluation of the slope  $\beta$  requires a specification of the relationship  $F = f(Q)$  and the use of statistical regression analysis [Kleinbaum and Kupper (1978); Johnston (1984)]. In what follows a possible relationship between  $F$  and  $Q$  is assumed and a methodology for statistical estimation of  $\beta$  is developed.

a. Functional relationship between  $F$  and  $Q$ . The scatter diagrams in Figures 4.1, 4.2, and 4.3 show that in observations on each sample the value of  $F$  at a certain value of  $Q$  is not consistent. This is due to the fact that random errors impart bias to the observation on  $F$ . In fact, the distribution of  $F$  at the same value of  $Q$  depends upon the statistical distribution of the random error. Thus, there is a whole probability distribution of values of  $F$  for each value of  $Q$ . The

scatter diagrams further suggest that the variation in the mean of  $F$  values at some  $Q$  is approximately linear with  $Q$ . Thus, a stochastic linear relationship between  $F$  and  $Q$  can be assumed. This stochastic linear relationship would become deterministic if the variance of  $F$  were zero; i.e., if there were no random errors in observations of  $F$ . The stochastic relationship between  $F$  and  $Q$  for  $n$  observations is:

$$F_i = \alpha + \beta Q_i + \epsilon_i \quad i = 1, 2, \dots, n \quad (4.2)$$

where the observed frequency  $F_i$  is taken to be the dependent variable, the number of maxima  $Q_i$  is the independent variable, and  $\epsilon$  is the stochastic disturbance,  $\alpha$  and  $\beta$  are the regression parameters. The values of  $F_i$  and  $Q_i$  are observable but those of  $\epsilon_i$  are not. The purpose of the  $\epsilon_i$  term is to characterize the discrepancies that emerge between the actual observed values of  $F$  and the values that would have been given by an exact functional relationship of the form:

$$F = \alpha + \beta Q . \quad (4.3)$$

The fact that the magnitude of  $\epsilon_i$  cannot be determined exactly means that the value of  $F$  can never be forecast with certainty, i.e., with probability 1. The uncertainty concerning  $F_i$  arises due to the presence of the stochastic disturbances  $\epsilon_i$  which, being random, imparts randomness to  $F_i$ . The randomness in the term  $\epsilon_i$  may be on account of a variety of factors which may or may not all be quantifiable. Among those factors are random apparatus or human ones as well as systematic errors in measurement of  $F$ ,  $L$ , and  $Q$ . The net effect of all such

factors, then, is summarized by a single stochastic variable  $\epsilon_i$ . The probability distribution of  $F$  and its properties are then determined by the values of  $Q$  and by the probability distribution of  $\epsilon$ . Thus, the full description of the model in Equation (4.2) also calls for the full specification of the probability distribution of the error  $\epsilon_i$ . We make the following statistical assumptions:

1.  $\epsilon_i$  is normally distributed  $\forall i$ .
2.  $\epsilon_i$  has zero mean, i.e.,  $\langle \epsilon_i \rangle = 0 \forall i$ .
3.  $\epsilon_i$  is homoskedastic, i.e.,  $\langle \epsilon_i^2 \rangle = \sigma^2$ . This means that every disturbance has the same variance  $\sigma^2$  for all observations whose value is unknown. This assumption rules out, for example, the possibility that the disturbance could be greater for higher values of  $Q$  than for lower values of  $Q$ .
4.  $\epsilon_i$  is nonautoregressive; i.e.,  $\langle \epsilon_i \epsilon_j \rangle = 0$  if  $i \neq j$ . This assumption implies that the expected value of  $F$  at any time in an experiment will be different from the expected value of  $F$  in the same experiment at a different time.
5.  $Q_i$  is a nonstochastic variable with values fixed in repeated sets of observations such that for any sample size  $n$   $\frac{1}{n} \sum_{i=1}^n (Q_i - \bar{Q})^2$  is a finite number where  $\bar{Q}$  is the mean value of  $Q$ .

With these assumptions, we can find the properties of the probability distribution of  $F_i$  for all  $i$ . The mean of  $F_i$  is obtained by taking the mathematical expectation value of both sides of Eq. (4.2):

$$\langle F_i \rangle = \langle \alpha + \beta Q_i + \epsilon_i \rangle . \quad (4.4a)$$

Since the expected value of  $\epsilon_i$  vanishes; i.e.,  $\langle \epsilon_i \rangle = 0$ , then

$$\langle F_i \rangle = \langle \alpha + \beta Q_i \rangle . \quad (4.4b)$$

The variance of  $F_i$  is

$$\begin{aligned} \text{Var}(F_i) &= \langle [F_i - \langle F_i \rangle]^2 \rangle \\ &= \langle [(\alpha + \beta Q_i + \epsilon_i) - (\alpha + \beta Q_i)]^2 \rangle \\ &= \langle \epsilon_i^2 \rangle = \sigma^2 . \end{aligned} \quad (4.5)$$

Equation (4.4b), which gives the mean value of  $F$  for each value of  $Q$ , is known as the population regression line. The slope  $\beta$  measures the change in the mean value of  $F$  corresponding to a unit change in the value of  $Q$ .

Estimation of the values of  $\alpha$  and  $\beta$  gives the sample regression line that serves as an estimate of the population regression line. If  $\alpha$  and  $\beta$  are estimated by  $\hat{\alpha}$  and  $\hat{\beta}$ , respectively, then the sample regression line is

$$\hat{F}_i = \hat{\alpha} + \hat{\beta} Q_i \quad (4.6)$$

where  $\hat{F}_i$  is the estimate of  $F_i$  or the fitted value of  $F_i$ . The observed values of  $F_i$  does not necessarily lie exactly on the sample regression line so that the value of  $F_i$  and  $\hat{F}_i$  in general are different. This difference is called the residual and is denoted by  $e_i$ . Thus we distinguish between the following:

$$\begin{aligned}
 F_i &= \alpha + \beta Q_i + \epsilon_i && \text{(population) ,} \\
 F_i &= \hat{\alpha} + \hat{\beta} Q_i + e_i && \text{(sample) .}
 \end{aligned}
 \tag{4.7}$$

In general, the residual  $e_i$  is different from  $\epsilon_i$  because  $\hat{\alpha}$  and  $\hat{\beta}$  are different from the true values of  $\alpha$  and  $\beta$ . In fact,  $e_i$  is the estimate of the disturbance  $\epsilon_i$ . Figure 4.4 is a schematic representation of this distinction. The slope  $\beta$  is obtained from Eq. (4.6):

$$\frac{d\hat{F}_i}{dQ} = \frac{\Delta\hat{F}}{\Delta Q} = \beta .
 \tag{4.8}$$

b. Evaluation of intercept  $\alpha$  and slope  $\beta$ .  $\alpha$  and  $\beta$  are estimated using ordinary least squares. If each residual  $e_i$  is squared, negative signs disappear, and the sum of squared residuals is a nonnegative quantity. In using the least square principle one selects  $\alpha$  and  $\beta$  for minimum  $\sum e_i^2$ . First, one evaluates

$$e_i = F_i - \hat{F}_i = F_i - (\hat{\alpha} + \hat{\beta} Q_i) ,$$

$$\sum e_i^2 = \sum (F_i - \hat{\alpha} - \hat{\beta} Q_i)^2 .$$

The necessary conditions for a stationary minimum are:

$$\begin{aligned}
 \frac{\partial \sum e_i^2}{\partial \hat{\alpha}} &= 0 , \\
 \frac{\partial \sum e_i^2}{\partial \hat{\beta}} &= 0 .
 \end{aligned}
 \tag{4.9}$$

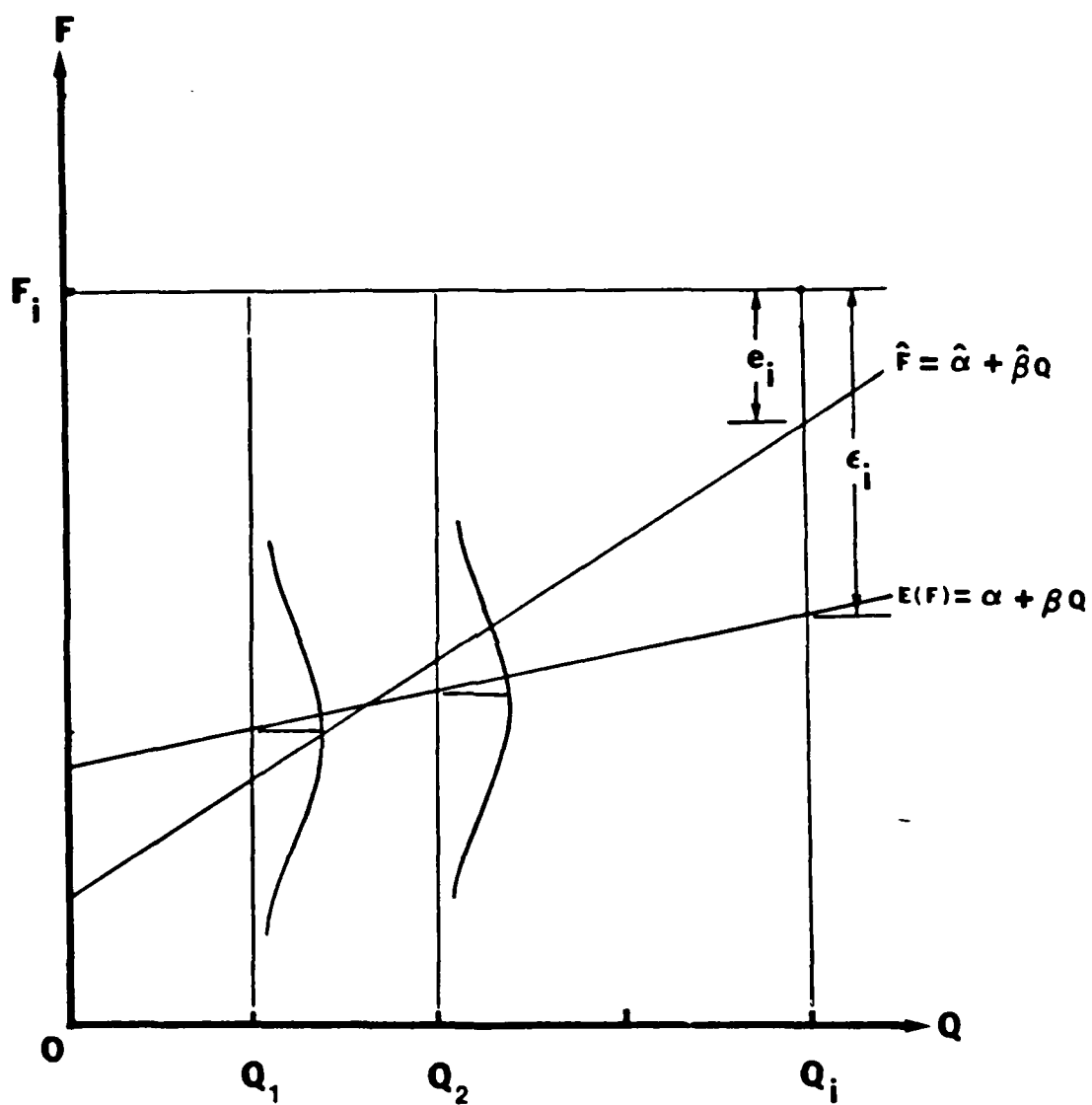


Figure 4.4. Schematic representation of population line  $E(F) = \alpha + \beta Q$  and sample line  $\hat{F} = \hat{\alpha} + \hat{\beta}Q$ .

It follows that:

$$\sum F_i = n\hat{\alpha} + \hat{\beta} \sum Q_i$$

where  $n$  is the number of data points. Since  $nQ_i = \sum_i Q_i$ , the product

$$\sum_{i=1}^n F_i Q_i = \hat{\alpha} \sum_{i=1}^n Q_i + \hat{\beta} \sum_{i=1}^n Q_i^2.$$

In matrix form this becomes

$$\begin{pmatrix} \hat{\alpha} \\ \hat{\beta} \end{pmatrix} = \begin{pmatrix} n & \sum Q_i \\ \sum Q_i & \sum Q_i^2 \end{pmatrix}^{-1} \begin{pmatrix} \sum F_i \\ \sum F_i Q_i \end{pmatrix}.$$

Evaluating the elements of the matrix, one obtains

$$\hat{\alpha} = \frac{1}{n} \sum F_i - \hat{\beta} \frac{1}{n} \sum Q_i, \quad (4.10a)$$

and

$$\hat{\beta} = \frac{\sum (Q_i - \bar{Q})(F_i - \bar{F})}{\sum (Q_i - \bar{Q})^2}. \quad (4.10b)$$

The quantities  $\hat{\alpha}$  and  $\hat{\beta}$  are, respectively, the intercept and the slope of the regression line. The slope  $\hat{\beta}$  is used to calculate the mean value of the velocity reported in this thesis.

## 2. Use of Data in Ordinary Least Squares Estimates of $\beta$ and Velocities

a. Computer program. A computer program for evaluating the regression line is available at The University of Tennessee Computer Center. This program, SYSREG, presented in Appendix A, was used to

evaluate the sample regression lines as in Equation (4.7). Values of  $\hat{\alpha}$  and  $\hat{\beta}$  evaluated from this regression line customarily are presented as follows:

$$\hat{F}_i = \hat{\alpha} + \hat{\beta}Q_i \quad R^2 = \dots \quad (4.11)$$

(S <sub>$\hat{\alpha}$</sub> ) (S <sub>$\hat{\beta}$</sub> )

where  $S_{\hat{\alpha}}^2$  is the estimate of variance of  $\hat{\alpha}$  and  $S_{\hat{\beta}}^2$  is the estimate of variance of  $\hat{\beta}$ .  $R^2$  is the coefficient of determination which is a measure of "goodness of fit"; i.e., how well the sample regression line fits the observations.  $R^2$  indicates the proportion of variation of  $F$  that can be attributed to the variation of  $Q$ . It is evaluated from

$$R^2 = \frac{\text{Regression Sum of Squares}}{\text{Total Sum of Squares}}$$

$$= 1 - \frac{\sum e_i^2}{\sum (F_i - \bar{F})^2}.$$

$R^2$  takes on the values:  $0 \leq R^2 \leq 1$ . A zero value of  $R^2$  indicates the poorest and a unit value the best fit that can be attained.

b. Velocities in germanium. The estimated regression lines obtained by applying the ordinary least squares estimate to data on the samples Ge(111), Ge(110), and Ge(100) are shown in standard form in Table 4.5. Note that the value of  $R^2$  in all the three orientations is close to unity which indicates that the data are well fit by the regression lines. The results are repeated in more detail in Table 4.6,

Table 4.5. Estimated Regression Lines for Ge[100], Ge[110], and Ge[111]

Sample	Estimated Regression Line
Ge(100)	$F_i = 27.8650 + 0.0660 Q_i + e_i$ , $R^2 = 0.9986$ (0.0133      (0.0002)
Ge(110)	$F_i = 24.916158 + 0.1118 Q_i + e_i$ , $R^2 = 0.9996$ (0.0134)      (0.0003)
Ge(111)	$F_i = 25.7741 + 0.05694 Q_i + e_i$ , $R^2 = 0.9992$ (0.0134)      (0.000156)

Table 4.6. Estimated Velocity in Present Experiment and Velocity Reported by McSkimin

Sample	$\alpha$	$S_{\alpha}$	$\hat{\beta} = \frac{\Delta \hat{f}}{\Delta Q}$	$S_{\hat{\beta}}$	Present Experiment $v = 2Ls\hat{\beta}$ (cm/sec)	McSkimin <sup>b</sup> (cm/sec)
Ge(100)	27.8650	0.0133	0.0660	0.0002	$4.9632 \times 10^5 \pm 0.80\%$ <sup>a</sup>	$4.9138 \times 10^5 \pm .02\%$ <sup>c</sup>
Ge(110)	24.916158	0.013461	0.111863	0.000301	$5.369 \times 10^5 \pm 0.52\%$ <sup>a</sup>	$5.4 \times 10^5 \pm .02\%$ <sup>c</sup>
Ge(111)	25.7741	0.0134	0.05694	0.000156	$5.5916 \times 10^5 \pm .53\%$ <sup>a</sup>	$(5.5585 \times 10^5)^d \pm .02\%$ <sup>c</sup>

<sup>a</sup>With 95% probability.

<sup>b</sup>Source: McSkimin, 1963.

<sup>c</sup>Probability level not indicated.

<sup>d</sup>Calculated by combining McSkimin's data.

where  $\hat{\alpha}$  is the intercept of the estimated regression line,  $\hat{\beta}$  is the slope,  $S_{\hat{\alpha}}$  and  $S_{\hat{\beta}}$  are the standard deviations in the measurements of  $\hat{\alpha}$  and  $\hat{\beta}$ .

### 3. Comparison of Results with Reference Values

The comparison of the results of the present measurements presented in Table 4.6 with those of McSkimin (also presented in Table 4.6) is especially informative. The present data present the scatter resulting from all sources of error, both definable and undefinable. Among the definable sources of error are systematic errors resulting from measurement of sample length, resonant frequency, and density. Random errors from repetition of these measurements also enter.

a. Evaluation of scatter of data around the mean. The results on velocity reported in Table 4.6 give the deviation of velocity values from the mean for a 95% probability level. The specification of the probability level gives a more complete picture of the effect of random errors on the data than usually is given. In Table 4.6 our estimated velocity in Ge[111] falls in the interval  $\pm 0.53\%$  of the mean value of velocity with a 95% probability. McSkimin reported a mean square deviation of  $\pm 0.02\%$ . It is apparent that our mean square deviation is larger than McSkimin's, but the significance of this statement is somewhat difficult to evaluate without information about his probability level. Further, whether the difference results from

our consideration of all sources of random error while McSkimin considered only errors resulting from diffraction is equally uncertain. Comparison of the remaining data in Table 4.6 results in similar conclusions.

b. Comparison of our mean value of velocity with values given by McSkimin. It remains to compare the mean value of velocity in this experiment with the values of velocity given by McSkimin. Agreement between the two sets of values adds credibility to the results. We let the three velocities in a germanium crystal as measured by McSkimin be  $v_{111}$ ,  $v_{110}$  and  $v_{100}$ . Somewhat at random, we chose the velocity in the [111] direction for our discussion of the comparison. (The comparison for the [110] and [100] directions is obtained by using velocity values appropriate to those directions.) Corresponding to McSkimin's value  $v_{111}$ , we evaluate the slope

$$\beta_{111} = \frac{v_{111}}{2Ls} . \quad - \quad (4.12)$$

To test whether the velocity estimated in this study is equal to that of McSkimin, we have to test whether our  $\hat{\beta}$  is equal to  $\beta_{111}$ . Therefore, we set the null hypotheses,\*

$$H_0: \hat{\beta} = \beta_{111}.$$

---

\*A null hypothesis is a proposition which is considered valid unless evidence throws serious doubt on it.

Equivalently,

$$H_0: v = v_{111}.$$

The T-statistic for the [111] direction is the function

$$\frac{\hat{\beta} - \beta_{111}}{S_{\hat{\beta}}}.$$

The distribution of the T-statistic about zero, known as the t-distribution, has  $(n-2)$  degrees of freedom. In estimating  $F$  one has two unknowns  $\hat{\alpha}$  and  $\hat{\beta}$  whose presence reduces the number of degrees of freedom from  $n$ , the total number of observations, to  $n-2$ . Let the significance level (unity minus the probability) be designated  $\lambda$ . Then, for a specified significance level  $\lambda$ , the T-statistic lies between the lower limit and the upper limit of a critical region as follows:

$$-t_{n-2, \lambda/2} \leq \frac{\hat{\beta} - \beta_{111}}{S_{\hat{\beta}}} \leq t_{n-2, \lambda/2} \quad (4.13)$$

The critical region is shown in Figure 4.5 with the limits specified.

Without the limits the t-distribution would vary from  $-\infty$  to  $\infty$ . In that case the cumulative probability would be unity; i.e., the area under the density function  $f\left(\frac{\hat{\beta} - \beta_{111}}{S_{\hat{\beta}}}\right)$  is unity. For a significance level  $\lambda$  the area under the distribution function is the probability

$$P = \int_{-t_{n-2, \lambda/2}}^{t_{n-2, \lambda/2}} f\left(\frac{\hat{\beta} - \beta_{111}}{S_{\hat{\beta}}}\right) d\left(\frac{\hat{\beta} - \beta_{111}}{S_{\hat{\beta}}}\right)$$

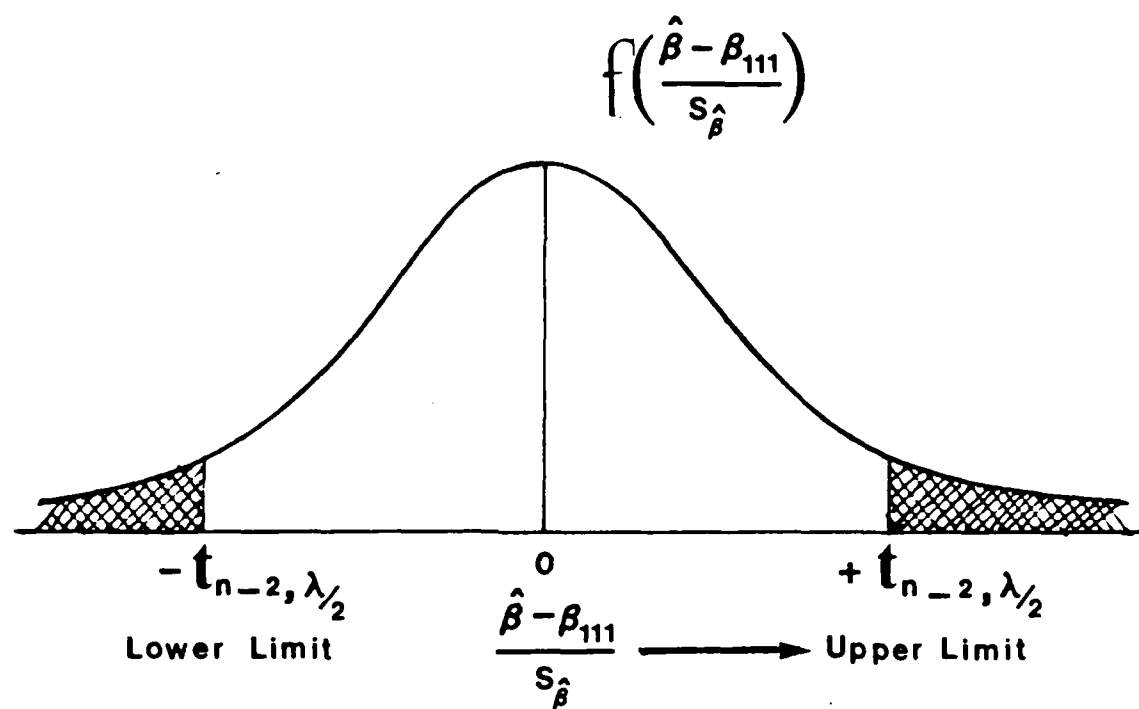


Figure 4.5. Distribution of  $f\left(\frac{\hat{\beta} - \beta_{111}}{s_{\hat{\beta}}}\right)$ .

which usually is designated as follows:

$$P = \left( -t_{n-2, \lambda/2} \leq \frac{\hat{\beta} - \beta_{111}}{S_{\hat{\beta}}} \leq t_{n-2, \lambda/2} \right) = 1 - \lambda. \quad (4.14)$$

The subscripts on the limits include  $\lambda/2$  because an area of  $\lambda/2$  is found on each tail of the t-distribution between  $t_{n-2, \lambda/2}$  and  $\infty$ . These areas can be read from t-distribution tables in statistics textbooks [Kleinbaum and Kupper (1978)]. For data in this thesis a value  $\lambda = 1\%$  is chosen, meaning that the area of the two tails is 0.5% each. The corresponding critical region and the T-statistic for the three crystalline modes are evaluated and are reported in Table 4.7.

From the inequality (4.13) we have

$$\beta_{111} - S_{\hat{\beta}} t_{n-2, \lambda/2} \leq \hat{\beta} \leq \beta_{111} + S_{\hat{\beta}} t_{n-2, \lambda/2}. \quad (4.15)$$

The above inequality gives the lower and upper limits of  $\hat{\beta}$  for the chosen significance level  $\lambda$ . The corresponding lower and upper limits of the estimated velocity  $v$  are found from (4.15) by multiplying the inequality by a factor  $2L_s$ :

$$v_{111} - 2L_s \cdot t_{n-2, \lambda/2} \cdot S_{\hat{\beta}} \leq v \leq v_{111} + 2L_s \cdot t_{n-2, \lambda/2} \cdot S_{\hat{\beta}}. \quad (4.16)$$

In terms of a percentage of  $v_{111}$ , we have:

$$\begin{aligned} v_{111} - \left( 2L_s \frac{t_{n-2, \lambda/2} \cdot S_{\hat{\beta}}}{v_{111}} \times 100 \right) v_{111} \leq v \leq v_{111} \\ + \left( 2L_s \frac{(t_{n-2, \lambda/2} \cdot S_{\hat{\beta}})}{v_{111}} \times 100 \right) v_{111} \end{aligned} \quad (4.17a)$$

Table 4.7. Comparison of Velocities in Present Experiment with Those of McSkimin

Sample	Velocity (McSkimin) $v_{100}, v_{110}, v_{111}$ (cm/sec)	$\beta = \frac{v}{2Ls}$	Velocity v (Present Experiment)* (cm/sec)	T-Statistic $\pm t_{n-2, \lambda/2}$	Critical Region	Variation $\Delta v$	Probability
Ge[100]	$4.9138 \times 10^5 \pm 0.015\%$	$\beta_{100} = 0.6527 \times 10^5$	$4.9684 \times 10^5 \pm 0.80\%$	2.50	2.639	0.71%	99%
Ge[110]	$5.40 \times 10^5 \pm 0.015\%$	$\beta_{110} = 1.125 \times 10^5$	$5.369 \times 10^5 \pm 0.52\%$	-2.114	2.656	0.7%	99%
Ge[111]	$5.55 \times 10^5 \pm 0.015\%$	$\beta_{111} = 0.566 \times 10^5$	$5.591 \times 10^5 \pm 0.53\%$	2.15	2.624	0.72%	99%

\*Probability level: 95%.

or

$$v_{111} - \Delta v_{111} \leq v \leq v_{111} + \Delta v_{111} \quad (4.17b)$$

where

$$\Delta v_{111} = \left\{ 2Ls \frac{t_{n-2, \lambda/2}}{v_{111}} \times 100 \right\} v_{111} .$$

Similar results are evaluated for the other two crystalline modes. The results are presented in Table 4.7, column 7. The associated probabilities are calculated from (4.14) and the results are presented in Table 4.7, column 8.

From the results reported in Table 4.7 we find that for  $\lambda = 1\%$  or for a probability level 99% the T-statistic does not exceed the critical region for all the three crystalline modes. As long as the T-statistic is within the critical region for a specified significance level, we do not reject the null hypothesis and conclude that there is not enough evidence to suggest that  $\hat{\beta}$  is different from  $\beta_{111}$ , or that the equivalently estimated velocity  $v$  is different from McSkimin's velocity  $v_{111}$ . In other words, the deviation of  $v$  around  $v_{111}$  will be confined to upper and lower limits  $v_{111} \pm \Delta v_{111}$  for 99% of the time. Only 1% of the time the deviation of  $v$  from  $v_{111}$  will be large enough so as to fall outside the limits  $v_{111} \pm \Delta v_{111}$ . Similar or better results are obtained for the other two crystalline modes. Thus we may conclude that the estimates of velocity in our experiment are in agreement of those of McSkimin. The results add credibility to our experiment and results as well as McSkimin's results.

#### 4. Error Propagation

In this section we compare the relative error in estimation of velocity in the present study with the error obtained by recombining values of elastic constants measured by others and using the expression  $K_2 = \rho v^2$ .

a. Error propagation in the present experiment. To derive a formula for the percentage error in the velocity one uses the expression for the regression line (Eq. 4.7).

$$F_i = \hat{\alpha} + \hat{\beta}Q_i + e_i, \quad (4.18)$$

where  $i = 1, 2, \dots, n$ . After applying a least squares analysis the fitted value of  $F_i$  is

$$\hat{F}_i = \hat{\alpha} + \hat{\beta}Q_i. \quad (4.19)$$

The mean values of  $F_i$  and  $Q_i$  also fit the regression line. Therefore, we have

$$\bar{F} = \hat{\alpha} + \hat{\beta}\bar{Q}, \quad (4.20)$$

where  $\bar{F}$  and  $\bar{Q}$  are the mean values of the observations taken in the experiment for a particular crystalline mode. These values are given as follows:

$$\bar{F} = \frac{1}{n} \sum_{i=1}^n F_i$$

and

$$\bar{Q} = \frac{1}{n} \sum_{i=1}^n Q_i .$$

From Eq. (4.20),

$$\hat{\beta} = \frac{\bar{F} - \hat{\alpha}}{\bar{Q}} .$$

Taking the logarithm of both sides and evaluating the partial derivatives:

$$\frac{\partial \hat{\beta}}{\hat{\beta}} = \frac{\partial (\bar{F} - \hat{\alpha})}{(\bar{F} - \hat{\alpha})} - \frac{\partial \bar{Q}}{\bar{Q}} \quad (4.21)$$

Evaluation of the relative errors requires consideration of the absolute value of each term:

$$\frac{\delta \hat{\beta}}{\hat{\beta}} = \left| \frac{\delta (\bar{F} - \hat{\alpha})}{(\bar{F} - \hat{\alpha})} \right| + \left| \frac{\delta \bar{Q}}{\bar{Q}} \right| \quad (4.22)$$

Since  $v = 2Ls\beta$ , the relative error in velocity is:  $\frac{\delta v}{v} = \frac{\delta \hat{\beta}}{\hat{\beta}}$  as  $L$  and  $s$  are constants. Therefore,

$$\frac{\delta v}{v} = \frac{\delta \bar{F} - S \hat{\alpha}}{\bar{F} - \hat{\alpha}} + \frac{\delta \bar{Q}}{\bar{Q}} \quad (4.23)$$

where the identity  $S_{\alpha}^{\wedge} = S_{\alpha}$  has been used. This formula is used to evaluate errors in the measurement of velocity due to random causes for all three samples and the results are presented in Table 4.8.

The error largely depends upon the value of the mean  $\bar{F}$ . The larger the value of  $\bar{F}$ , the smaller the percentage error. The error in Ge (111) is much smaller than the error in Ge (100) because it was possible to obtain a larger number of measures  $Q_i$  in the Ge (111) sample, and hence to have a larger value of  $\bar{F}$ . The experimenter does not always have total control over the value of  $\bar{F}$ , but should always seek to obtain the largest value possible.

b. Error propagation in use of reference values of  $C_{ij}$ . The percentage error found in the preceding section now is compared with the error propagated when one takes the values of the second-order constants from reference sources (McSkimin, 1963) and calculates the velocity of longitudinal waves in the three principal directions using the following formulae:

$$v_{100}^2 = C_{11}/\rho \quad (4.24a)$$

$$v_{110}^2 = (C_{11} + C_{12} + 2C_{44})/2\rho \quad (4.24b)$$

$$v_{111}^2 = (C_{11} + 2C_{12} + 4C_{44})/3\rho \quad (4.24c)$$

in which the combinations of second-order elastic constants are recognized as being the same as the  $K_2$ 's listed in Table 1.1, p. 4).

The relative errors in the velocities are:

Table 4.8. Propagated Error ( $\delta v/v$ ) in Present Experiment

Sample	Propagated Error ( $\delta v/v$ )
Ge[100]	0.46%
Ge[110]	0.33%
Ge[111]	0.29%

$$\frac{\delta v_{100}}{v_{100}} = \frac{1}{2} \frac{\delta C_{11}}{C_{11}} + \frac{1}{2} \frac{\delta \rho}{\rho} \quad (4.25a)$$

$$\frac{\delta v_{110}}{v_{110}} = \frac{1}{2} \left( \frac{\delta C_{11} + \delta C_{12} + 2\delta C_{44}}{C_{11} + C_{12} + 2C_{44}} \right) + \frac{1}{2} \frac{\delta \rho}{\rho} \quad (4.25b)$$

$$\frac{\delta v_{111}}{v_{111}} = \frac{1}{2} \frac{\delta C_{11} + 2\delta C_{12} + 4\delta C_{44}}{C_{11} + 2C_{12} + 4C_{44}} + \frac{1}{2} \frac{\delta \rho}{\rho} \quad (4.25c)$$

Using these equations and the values for the errors given in the reference and assuming an error in the measurement of  $\rho$  as 0.1%, the propagated errors are calculated and are given in Table 4.9.

#### 5. Correction of Systematic Error

Close examination of the data in Tables 4.2, 4.3, and 4.4 (pp. 28, 29, 30) presented in the scatter diagrams in Figures 4.1, 4.2, and 4.3 (pp. 31, 32, 33) reveals systematic errors in some of the data. Some of the numbers appear to deviate by more than one standard deviation resulting from either an extra count or a missed count in the data taking. Such errors can be corrected by standard techniques. The data were subjected to analysis by a computer program to make such corrections. The results are given in Tables 4.10 and 4.11 which can be compared directly with Tables 4.6 and 4.7 (pp. 44, 50), respectively. Comparison reveals that both the slopes  $\hat{\beta}$  and the standard deviations  $S_{\hat{\beta}}$  were improved. The slopes were used to calculate present experiment values of the velocities  $v$  which are observed to be in better agreement with the measured data of McSkimin listed in Table 4.10, and the deviations from the mean velocity were reduced. In Table 4.11 it

Table 4.9. Propagated Error ( $\delta v/v$ ) from Standard Sources

Sample	Propagated Error ( $\delta v/v$ ) from Standard Results*
[100]	0.07%
[110]	0.07%
[111]	0.08%

\*These values have been calculated using the constants given in McSkimin (1963):

$$C_{11} = 12.8528 \times 10^{11} \pm 0.04\%$$

$$C_{22} = 4.8259 \times 10^{11} \pm 0.04\%$$

$$C_{44} = 6.67966 \times 10^{11} \pm 0.04\%$$

Figure 4.10. Corrected Estimates on Velocity in Present Experiment and Velocity Reported by McSkimin

Sample	$\alpha$	$S_{\hat{\alpha}}$	$\hat{\beta} = \frac{\Delta F}{\Delta Q}$	$S_{\hat{\beta}}$	Present Experiment $v = 2\lambda S_{\hat{\beta}}$ (cm/sec)	McSkimin <sup>b</sup> (cm/sec)
Ge(100)	27.8635	0.0078	0.065742	0.0001	$4.9461 \times 10^5 \pm 0.50\%$ <sup>a</sup>	$4.9138 \times 10^5 \pm .02\%$ <sup>c</sup>
Ge(110)	24.911860	0.012099	0.11216	0.000347	$5.449 \times 10^5 \pm 0.60\%$ <sup>a</sup>	$5.4 \times 10^5 \pm .02\%$ <sup>c</sup>
Ge(111)	25.7635	0.0045	0.0571	0.000053	$5.613 \times 10^5 \pm .18\%$ <sup>a</sup>	$(5.5585 \times 10^5)^d \pm .02\%$ <sup>c</sup>

<sup>a</sup>With 95% probability.

<sup>b</sup>Source: McSkimin, 1963.

<sup>c</sup>Probability level not indicated.

<sup>d</sup>Calculated by combining McSkimin's data.

Table 4.11. Comparison of Corrected Velocities in Present Experiment with Those of McSkimin

Sample	Velocity (McSkimin) $v_{100}, v_{110}, v_{111}$ (cm/sec)	$\beta = \frac{v}{2Ls}$	Velocity $v$ (Present Experiment)* (cm/sec)	T-Statistic	Critical Region, $\pm t_{n-2, /2}$	Variation $\Delta v$	Probability
Ge[100]	$4.9138 \times 10^5 \pm 0.02\%$	$\beta_{100} = 0.6530 \times 10^5$	$4.9461 \times 10^5 \pm 0.50\%$	2.36	2.639	0.68%	99%
Ge[110]	$5.40 \times 10^5 \pm 0.02\%$	$\beta_{110} = 1.111 \times 10^5$	$5.449 \times 10^5 \pm 0.60\%$	-2.80	2.656	0.81%	99%
Ge[111]	$5.550 \times 10^5 \pm 0.02\%$	$\beta_{111} = 0.565 \times 10^5$	$5.613 \times 10^5 \pm 0.18\%$	11.32	2.624	0.24%	99%

\*Probability level: 95%.

is found that the T statistic still lies within the critical region for the [100] and [110] values; however, the [111] T statistic now lies outside the critical region. This probably results from the fact that, as indicated, the [111] value was obtained from McSkimin's data by adding certain numbers to give a propagated error which has not been accounted for in the analysis. An additional possibility is that the present value of  $S_{\beta}$  of only 0.000053 results in an anomalously large T statistic. Finally, the variation  $\Delta v$  of the present data from those of McSkimin in all three cases is decreased by the correction of the systematic error.

The results presented in Tables 4.10 and 4.11 also have been calculated by including all of the significant figures in the lengths given in Table 4.1 (p. 27). Tables 4.6 and 4.7 (pp. 44, 50) were calculated by rounding off the lengths to three significant figures. Although the change in the velocities resulting from the more accurate value of length is not great, it was detectable in the fourth significant figure in the velocity. Hence, the correction is justified.

## CHAPTER V

### SUMMARY

The analysis in this thesis shows that the question originally posed does not have a unique answer for all samples under all conditions. One cannot decide a priori whether reference values of  $C_{ij}$  should be used or whether one should measure the  $C_{ij}$  each time he measures the  $C_{ijk}$ . The analysis given, however, tends to support the position that on those occasions one has data as accurate as those of McSkimin his accuracy is greatest if he uses them rather than remeasuring each sample. If such accurate data are not available, one has no choice.

## REFERENCES

## REFERENCES

- Bateman, T. B., W. P. Mason, and H. J. McSkimin, J. Appl. Phys. 32, 928 (1961).
- Breazeale, M. A., and John H. Cantrell, Jr., J. Acoust. Soc. Am. 61, 403 (1977).
- Breazeale, M. A., John H. Cantrell, Jr., and Joseph H. Heyman, "Ultrasonic Wave Velocity and Attenuation Measurements," Chap. 2 in Methods of Experimental Physics, Vol. 19, edited by Peter D. Edmonds. New York: Academic Press, 1981.
- Breazeale, M. A., and W. B. Gauster, Phys. Rev. 168, 655 (1968).
- Green, Robert E., Jr., Treatise on Material Science and Technology. New York: Academic Press, 1973.
- Holt, Albert C., and Joseph Ford, J. Appl. Phys. 38, 49 (1967).
- Johnston, J., Econometric Methods. New York: McGraw-Hill, 1984.
- Kleinbaum, David G., and Lawrence L. Kupper, Applied Regression Analysis and Other Multivariable Methods. North Scituate, MA: Duxbury Press, 1978.
- Lord Rayleigh. The Theory of Sound. New York: Dover Publications, 1945, Vol. II.
- McSkimin, H. T., and P. Andreatch, Jr., J. Appl. Phys. 34, 651 (1963).
- Murnaghan, F. D. Finite Deformation of an Elastic Solid. New York: John Wiley and Sons, 1951.
- Musgrave, M. J. P., Crystal Acoustics. San Francisco, Cambridge, London, Amsterdam: Holden-Day, 1970.
- Spiegel, M. R., Mathematical Handbook for Formulas and Tables. New York: McGraw-Hill, 1968.

APPENDIXES

## APPENDIX A

### THEORY OF PULSE SUPERPOSITION TECHNIQUE

The equation of motion for a progressive wave propagating in a medium is given by

$$u = Ae^{i(kx-\omega t)} \quad (A-1)$$

where  $A$  is the amplitude of the wave.

Let us consider two such progressive waves given by

$$\begin{aligned} u_1 &= A_1 e^{i(kx_1 - \omega t_1)} \\ u_2 &= A_2 e^{i(kx_2 - \omega t_2)} \end{aligned} \quad (A-2)$$

Consider the sample of length  $\ell$  as shown in Figure A.1. The electrical signal applied to the transducer bonded to the sample by means of stopcock grease causes the transducer to emit an ultrasonic wave which travels through the sample and is detected at the opposite end of the sample by the capacitive receiver. The signal is displayed on the oscilloscope screen. In this process the first pulse is detected when the ultrasonic wave reaches the end of the sample at the capacitive receiver. After this, the wave undergoes reflection, returns and once again is reflected. The second pulse thus seen on the oscilloscope screen accounts for the signal that is detected after the ultrasonic wave has undergone two reflections.

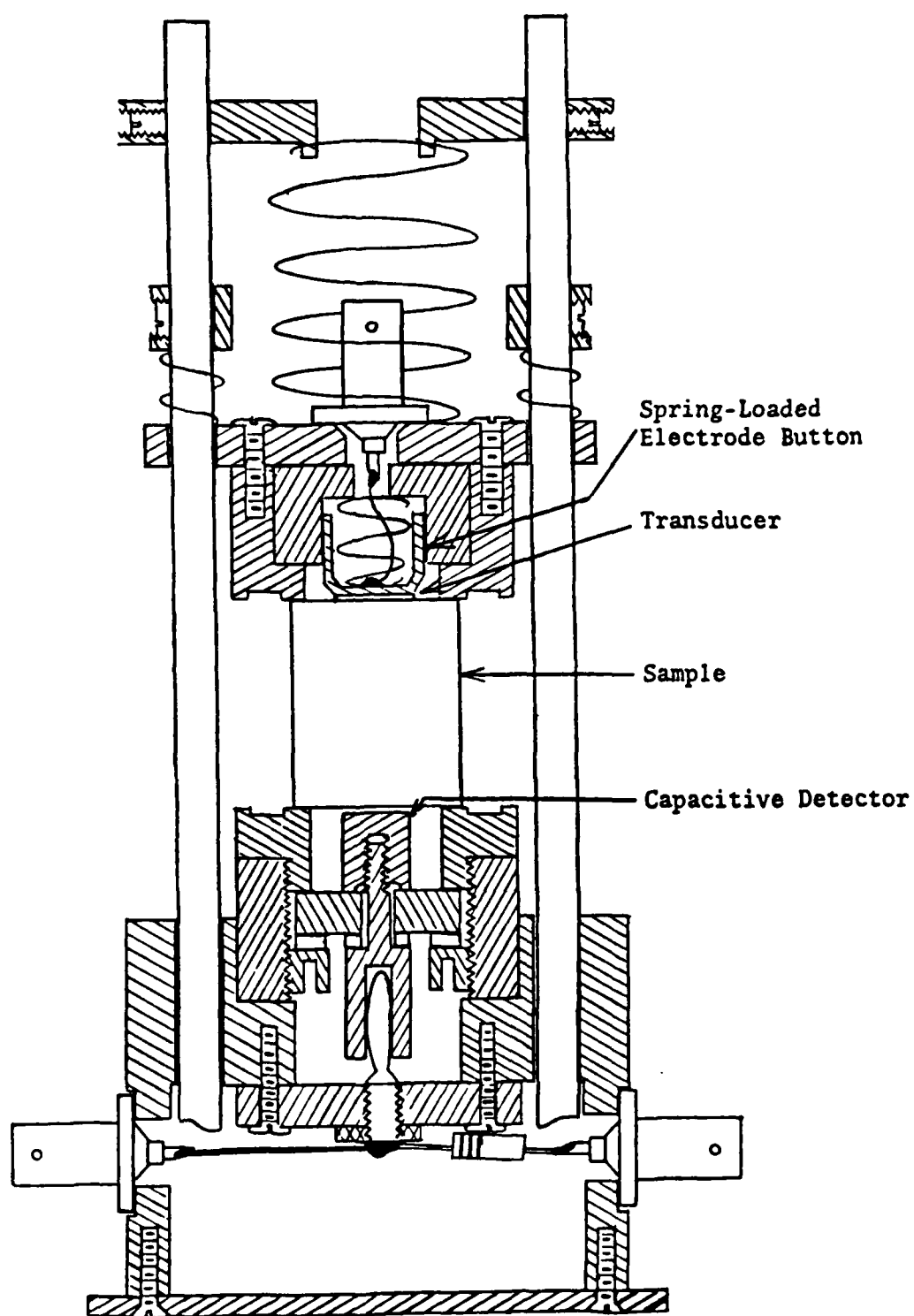
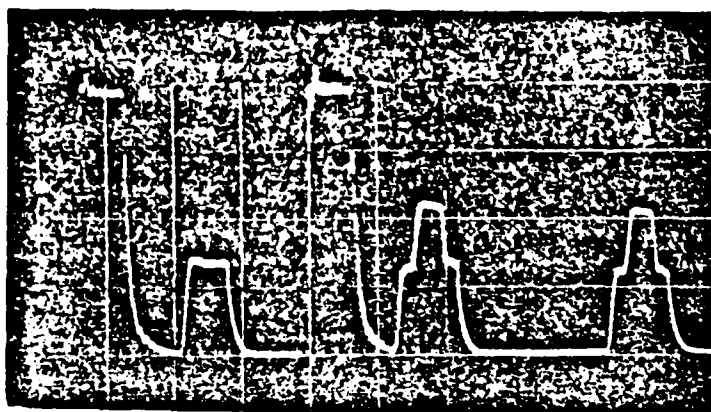
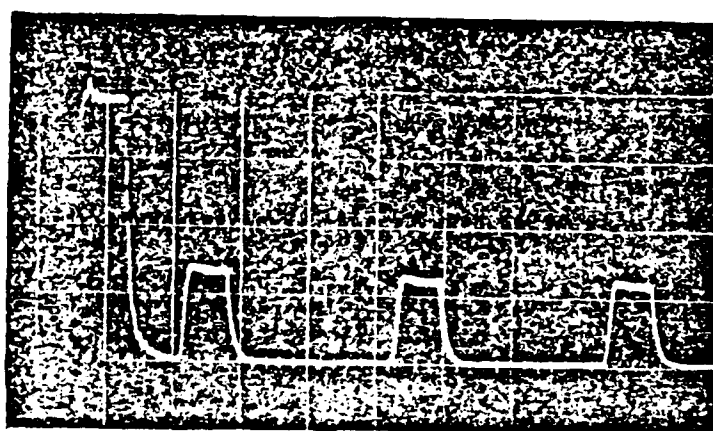


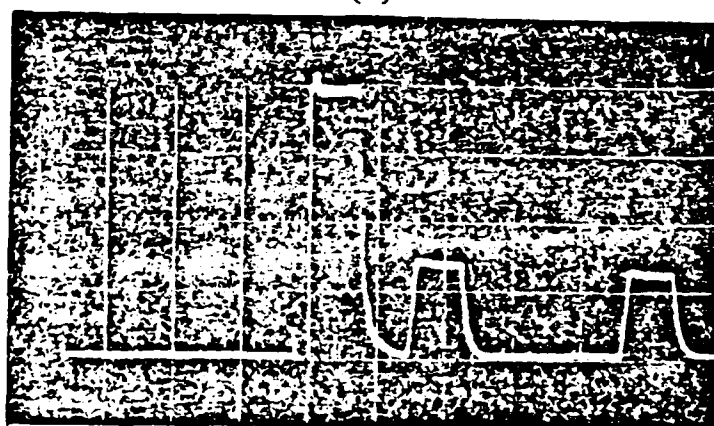
Figure A.1. Cross sectional view of the room temperature apparatus.



(a)



(b)



(c)

Figure A.2. (a) A typical interference pattern obtained with the pulse overlap technique; (b) and (c) show the separate pulse trains which interfere to give the pattern of (a).

Since the expression for the velocity of sound is derived upon the basic assumption that the wave has undergone two reflections before it is detected, the velocity formula derived below is valid for all pulses except the first pulse which is detected before two reflections. Therefore, for the first echo of some initial pulse which corresponds to the second pulse that is seen on the screen as shown in Figure A-2, one can write

$$x_1 = (x + 2\lambda) + \frac{2\phi}{k} . \quad (A-3)$$

The pulse travels the distance  $\lambda$ , is reflected at the sample surface and again travels a distance  $\lambda$ , whereupon it is reflected again at the boundary. After the second reflection, if it travels a distance  $x$ , as shown in Figure A-3, then the total distance traveled is  $(2\lambda + x)$ . In addition, since the wave undergoes two reflections, it also undergoes two phase changes which need to be accounted for. The distance corresponding to one phase change is  $\frac{\phi}{k}$ , where  $\phi$  is the phase change upon reflection. Since two phase changes are involved, the corresponding distance is given by  $\frac{2\phi}{k}$ . Therefore, the total distance traveled by the wave before the first echo is seen is given by the sum

$$x_1 = x + 2\lambda + \frac{2\phi}{k} .$$

If there are  $n$  such echoes, the expression takes the general form

$$x_1 = x + 2n\lambda + \frac{2n\phi}{k}$$

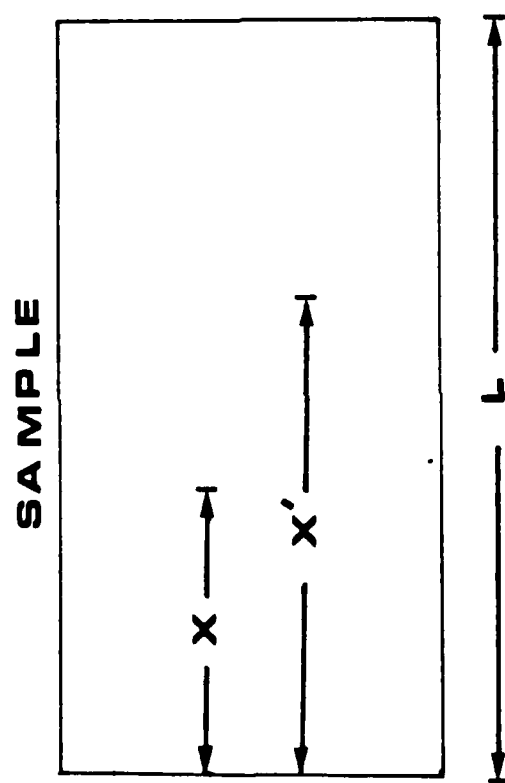


Figure A.3. Distances travelled by two pulses after undergoing two reflections at the boundaries of the sample.

for the  $n$ th echo. Similarly, for some other initial pulse (delayed in time with respect to the first pulse) for the  $m$ th echo, we have

$$x_2 = x' + 2m\lambda + \frac{2m\phi}{k} .$$

For overlap of echoes we require

$$x = x'$$

$$A_1 = A_2 = A$$

$$t_1 = t_2$$

and:

$$u = u_1 + u_2 = A_1 e^{i(kx_1 - \omega t_1)} + A_2 e^{i(kx_2 - \omega t_2)} . \quad (A-4)$$

Since

$$A_1 = A_2 = A$$

$$t_1 = t_2$$

and

$$x = x' ,$$

we have

$$u = A e^{i(kx - \omega t)} [e^{i(2nk\lambda + 2n\phi)} + e^{i(2mk\lambda + 2m\phi)}] . \quad (A-5)$$

Since the delayed pulse started later than the first one, we have

$n > m$ , so that one can write

$$n - m = s .$$

Substituting for  $n$  in terms of  $m$  and  $s$ , we have

$$u = Ae^{i(kx - \omega t)} [e^{i\{2(m+s)k\lambda + 2(m+s)\phi\}} + e^{i(2mk\lambda + 2m\phi)}] \quad (\text{A-6})$$

or

$$u = Ae^{i(kx - \omega t)} e^{i(2mk\lambda + 2m\phi)} [e^{i(2sk\lambda + 2s\phi)} + 1] . \quad (\text{A-7})$$

For destructive interference, we have the condition

$$2sk\lambda + 2s\phi = (2q + 1)\pi \quad (\text{A-8})$$

where  $q = 0, 1, 2, 3$ , or, since  $k = \frac{2\pi}{\lambda} = \frac{2\pi f\lambda}{v}$ ,

$$(2q + 1)\pi = 2s\phi + \frac{4\pi s f \lambda}{v} . \quad (\text{A-9})$$

If we change the driving frequency so that we go through destructive interferences, then we have for the beginning frequency  $f_1$ :

$$(2q_1 + 1)\pi + 2s\phi + \frac{4\pi s f_1 \lambda}{v} \quad (\text{A-10})$$

and for the final frequency  $f_2$ :

$$(2q_2 + 1)\pi = 2s\phi + \frac{4\pi s f_2 \lambda}{v} . \quad (\text{A-11})$$

Subtracting (A-10) from (A-11), we have

$$2(q_2 - q_1)\pi = \frac{4\pi s \lambda}{v} (f_2 - f_1) .$$

Letting  $q_2 - q_1 = \Delta q$  and  $f_2 - f_1 = \Delta f$  and solving for the wave velocity  $v$ , we have

$$v = 2s\lambda \frac{\Delta f}{\Delta q} ,$$

(A-12)

which has been used to interpret data in this thesis.

## APPENDIX B

### COMPUTER PROGRAM FOR COMPUTING VELOCITY

```
1 //SONIC JOB , ,GROUP= ,USER= ,TIME=(5,0),CLASS=T,  
  // PASSWORD=  
  ***JOBPARM LINES=5,CARDS=5000,ROOM=BIN4  
  ***ROUTE PRINT RMT26  
2 // EXEC SAS,REGION=512K  
23 //SYSIN DD *
```

NOTE: SAS OPTIONS SPECIFIED ARE:  
 SORT=4

```
1      OPTIONS LS=72;  
2      DATA SOUND;  
3      INPUT Q F;  
4      CARDS;
```

NOTE: DATA SET WORK.SOUND HAS 108 OBSERVATIONS AND 2 VARIABLES. 2346 OBS

NOTE: THE DATA STATEMENT USED 0.08 SECONDS.

```
113     PROC PRINT;  
114     TITLE OBSERVATIONS ON F AND Q FOR GE(111);
```

NOTE: THE PROCEDURE PRINT USED 0.17 SECONDS  
 AND PRINTED PAGES 1 TO 2.

```
115     PROC MEANS;  
116     TITLE STATISTICAL ANALYSIS FOR GE(111);
```

NOTE: THE PROCEDURE MEANS USED 0.13 SECONDS  
 AND PRINTED PAGE 3.

```
117     PROC SYSREG;MODEL F=Q;
```

NOTE: THE PROCEDURE SYSREG USED 0.15 SECONDS  
 AND PRINTED PAGE 4.

```
118     PROC PLOT;  
119     TITLE PLOT OF F VS. Q FOR GE(111);  
120     PLOT F*Q;
```

NOTE: THE PROCEDURE PLOT USED 0.16 SECONDS  
 AND PRINTED PAGE 5.

NOTE: SAS INSTITUTE INC.  
 SAS CIRCLE  
 PO BOX 8000  
 CARY, N.C. 27511-8000

OBSERVATIONS ON F AND Q FOR GE(111)  
14:14 THURSDAY, DECEMBER 5, 1985

GBS	Q	F
1	0	25.689
2	10	26.266
3	20	26.836
4	30	27.403
5	40	27.988
6	50	28.557
7	60	29.128
8	70	29.700
9	80	30.272
10	90	30.832
11	100	31.399
12	110	31.983
13	120	32.546
14	130	33.133
15	140	33.687
16	150	34.266
17	160	34.752
18	0	25.684
19	10	26.266
20	20	26.832
21	30	27.400
22	40	27.974
23	50	28.530
24	60	29.124
25	70	29.685
26	80	30.268
27	90	30.833
28	100	31.398
29	110	31.979
30	120	32.554
31	130	33.105
32	140	33.701
33	150	34.261
34	160	34.752
35	0	25.684
36	10	26.266
37	20	26.835
38	30	27.402
39	40	27.993
40	50	28.553
41	60	29.126
42	70	29.700
43	80	30.269
44	90	30.833
45	100	31.397
46	110	31.989
47	120	32.547
48	130	33.140
49	140	33.712
50	150	34.246
51	0	25.863
52	10	26.428
53	20	26.992
54	30	27.568

OBSERVATIONS ON F AND Q FOR GE(111)  
 14:14 THURSDAY, DECEMBER 5, 1985<sup>2</sup>

OBS	Q	F
55	40	28.144
56	50	28.714
57	60	29.302
58	70	29.865
59	80	30.429
60	90	30.995
61	100	31.564
62	110	32.150
63	120	32.714
64	130	33.296
65	140	33.817
66	0	25.863
67	10	26.425
68	20	26.996
69	30	27.568
70	40	28.155
71	50	28.744
72	60	29.301
73	70	29.865
74	80	30.430
75	90	30.998
76	100	31.581
77	110	32.146
78	120	32.717
79	130	33.303
80	140	33.811
81	0	25.792
82	10	26.373
83	20	26.943
84	30	27.497
85	40	28.068
86	50	28.652
87	60	29.228
88	70	29.801
89	80	30.376
90	90	30.938
91	100	31.503
92	110	32.085
93	120	32.673
94	130	33.235
95	140	33.801
96	0	25.792
97	10	26.318
98	20	26.889
99	30	27.481
100	40	28.036
101	50	28.610
102	60	29.183
103	70	29.779
104	80	30.318
105	90	30.886
106	100	31.452
107	110	32.043
108	120	32.625

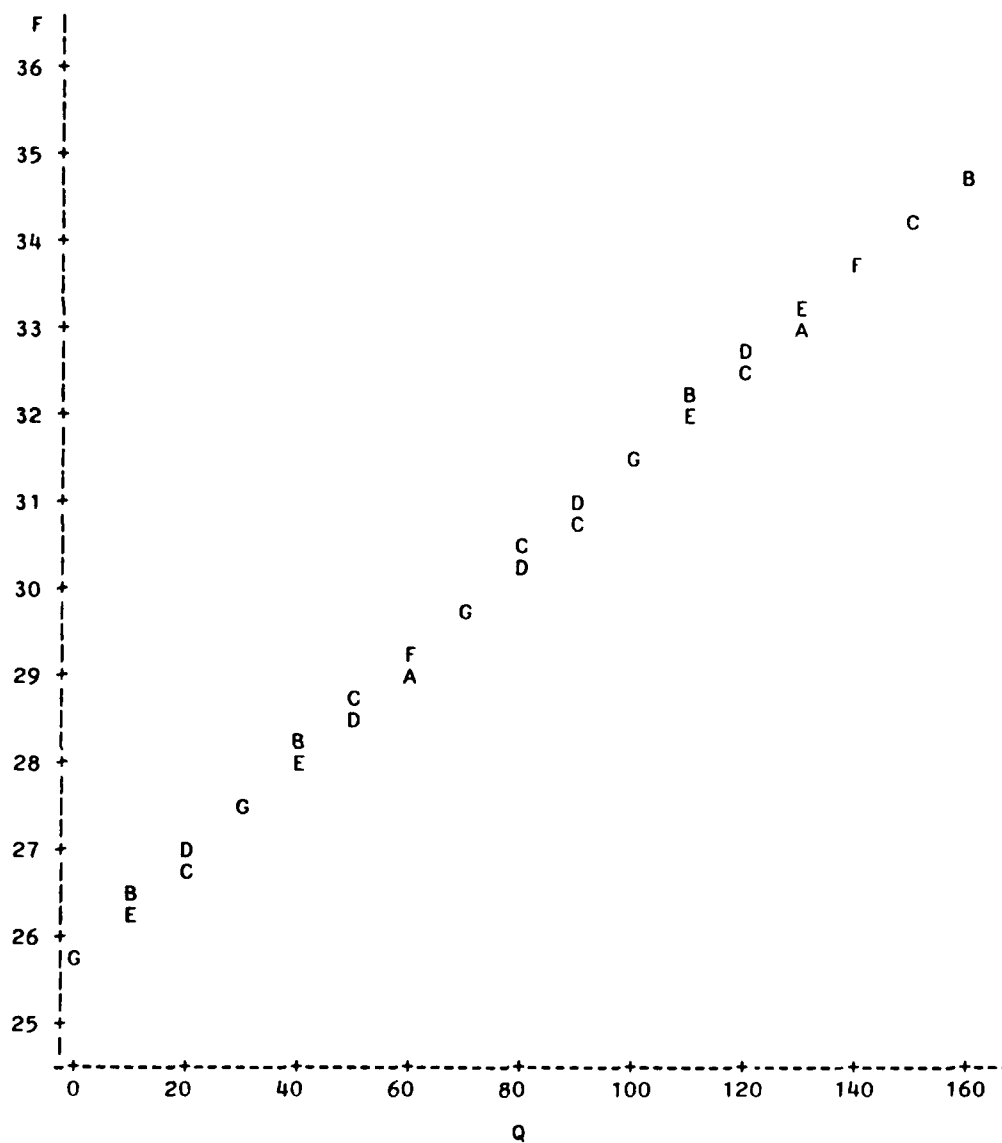
STATISTICAL ANALYSIS FOR GE(111) 3  
14:14 THURSDAY, DECEMBER 5, 1985

VARIABLE	N	MEAN	STANDARD DEVIATION	MINIMUM VALUE	MAXIMUM VALUE
Q	108	72.68518519	45.56204523	0.00000000	160.0000000
F	108	29.91292593	2.59537738	25.68400000	34.7520000

STATISTICAL ANALYSIS FOR GE(111)  
14:14 THURSDAY, DECEMBER 5, 1985<sup>4</sup>

MODEL:	MODEL01	SSE	0.576765	F RATIO	132356.05
		DFE	106	PROB>F	0.0001
DEP VAR:	F	MSE	0.005441183	R-SQUARE	0.9992
VARIABLE	DF	PARAMETER ESTIMATE	STANDARD ERROR	T RATIO	PROB> T
INTERCEPT	1	25.774174	0.013409	1922.1649	0.0001
Q	1	0.056941	0.0001565134	363.8077	0.0001

PLOT OF F VS. Q FOR GE(111)  
14:14 THURSDAY, DECEMBER 5, 1985  
PLOT OF F\*Q      LEGEND: A = 1 OBS, B = 2 OBS, ETC.



APRIL 1984

REPORTS DISTRIBUTION LIST FOR ONR PHYSICS DIVISION OFFICE  
UNCLASSIFIED CONTRACTS

Director Defense Advanced Research Projects Agency Attn: Technical Library 1400 Wilson Blvd. Arlington, VA 22209	1 copy
Office of Naval Research Physics Division Office (Code 1112) 800 North Quincy St. Arlington, VA 22217	2 copies
Office of Naval Research Director, Technology (Code 200) 800 North Quincy St. Arlington, VA 22217	1 copy
Naval Research Laboratory Department of the Navy Attn: Technical Library Washington, DC 20375	1 copy
Office of the Director of Defense Research and Engineering Information Office Library Branch The Pentagon Washington, DC 20301	1 copy
U.S. Army Research Office Box 1211 Research Triangle Park North Carolina 27709	2 copies
Defense Technical Information Center Cameron Station Alexandria, VA 22314	12 copies
Director, National Bureau of Standards Attn: Technical Library Washington, DC 20234	1 copy
Director U.S. Army Engineering Research and Development Laboratories Attn: Technical Documents Center Fort Belvoir, VA 22060	1 copy
ODDR&E Advisory Group on Electron Devices 201 Varick St. New York, NY 10014	1 copy

Air Force Office of Scientific Research Department of the Air Force Bolling AFB, DC 22209	1 copy
Air Force Weapons Laboratory Technical Library Kirtland Air Force Base Albuquerque, NM 87117	1 copy
Air Force Avionics Laboratory Air Force Systems Command Technical Library Wright-Patterson Air Force Base Dayton, OH 45433	1 copy
Lawrence Livermore Laboratory Attn: Dr. W. F. Krupke University of California P.O. Box 808 Livermore, CA 94550	1 copy
Harry Diamond Laboratories Technical Library 2800 Powder Mill Road Adelphi, MD 20783	1 copy
Naval Air Development Center Attn: Technical Library Johnsville Warminster, PA 18974	1 copy
Naval Weapons Center Technical Library (Code 753) China Lake, CA 93555	1 copy
Naval Underwater Systems Center Technical Center New London, CT 06320	1 copy
Commandant of the Marine Corps Scientific Advisor (Code RD-1) Washington, DC 20380	1 copy
Naval Ordnance Station Technical Library Indian Head, MD 20640	1 copy
Naval Postgraduate School Technical Library (Code 0212) Monterey, CA 93940	1 copy
Naval Missile Center Technical Library (Code 5632.2) Point Mugu, CA 93010	1 copy

Naval Ordnance Station Technical Library Louisville, KY 40214	1 copy
Commanding Officer Naval Ocean Research & Development Activity Technical Library NSTL Station, MS 39529	1 copy
Naval Explosive Ordnance Disposal Facility Technical Library Indian Head, MD 20640	1 copy
Naval Ocean Systems Center Technical Library San Diego, CA 92152	1 copy
Naval Surface Weapons Center Technical Library Silver Springs, MD 20910	1 copy
Naval Ship Research and Development Center Central Library (Code L42 and L43) Bethesda, MD 20084	1 copy
Naval Avionics Facility Technical Library Indianapolis, IN 46218	1 copy
Dr. Bill D. Cook Dept. of Mechanical Engineering University of Houston Houston, TX 77004	1 copy
Dr. Floyd Dunn Biophysical Research Laboratory University of Illinois Urbana, IL 61801	1 copy
Dr. E. F. Carome Department of Physics John Carroll University University Heights Cleveland, OH 44017	1 copy
Albert Goldstein, Ph.D. Dept. of Radiology Harper-Grace Hospitals 3990 John R. Detroit, MI 48201	1 copy

END

2-87

DTIC